Today's outline - November 11, 2024

Today's outline - November 11, 2024

- Final Project

Today's outline - November 11, 2024

- Final Project
- EXAFS Theory

Today's outline - November 11, 2024

- Final Project
- EXAFS Theory
- XAS Experiments

Today's outline - November 11, 2024

- Final Project
- EXAFS Theory
- XAS Experiments
- Photoemission

Today's outline - November 11, 2024

- Final Project
- EXAFS Theory
- XAS Experiments
- Photoemission

Reading Assignment: Chapter 8.4

Today's outline - November 11, 2024

- Final Project
- EXAFS Theory
- XAS Experiments
- Photoemission

Reading Assignment: Chapter 8.4

Homework Assignment #06:
Chapter 6: 1,6,7,8,9
due Friday, November 15, 2024

Today's outline - November 11, 2024

- Final Project
- EXAFS Theory
- XAS Experiments
- Photoemission

Reading Assignment: Chapter 8.4

Homework Assignment #06:
Chapter 6: 1,6,7,8,9
due Friday, November 15, 2024

Please send me your choices for General User proposal and final exam presentation. I need to approve them by the end of the week!

Final projects & presentations

In-class student presentations on research topics

Final projects & presentations

In-class student presentations on research topics

- Choose a research article which features a synchrotron technique

Final projects & presentations

In-class student presentations on research topics

- Choose a research article which features a synchrotron technique
- Get it approved by instructor first!

Final projects & presentations

In-class student presentations on research topics

- Choose a research article which features a synchrotron technique
- Get it approved by instructor first!
- Schedule a 20 minute time on Final Exam Day (Thursday, May 4, 2023, 17:00-19:00)

Final projects & presentations

In-class student presentations on research topics

- Choose a research article which features a synchrotron technique
- Get it approved by instructor first!
- Schedule a 20 minute time on Final Exam Day (Thursday, May 4, 2023, 17:00-19:00)

Final project - writing a General User Proposal

Final projects & presentations

In-class student presentations on research topics

- Choose a research article which features a synchrotron technique
- Get it approved by instructor first!
- Schedule a 20 minute time on Final Exam Day (Thursday, May 4, 2023, 17:00-19:00)

Final project - writing a General User Proposal

- Think of a research problem (could be yours) that can be approached using synchrotron radiation techniques

Final projects & presentations

In-class student presentations on research topics

- Choose a research article which features a synchrotron technique
- Get it approved by instructor first!
- Schedule a 20 minute time on Final Exam Day (Thursday, May 4, 2023, 17:00-19:00)

Final project - writing a General User Proposal

- Think of a research problem (could be yours) that can be approached using synchrotron radiation techniques
- Make proposal and get approval from instructor before starting

Final projects & presentations

In-class student presentations on research topics

- Choose a research article which features a synchrotron technique
- Get it approved by instructor first!
- Schedule a 20 minute time on Final Exam Day (Thursday, May 4, 2023, 17:00-19:00)

Final project - writing a General User Proposal

- Think of a research problem (could be yours) that can be approached using synchrotron radiation techniques
- Make proposal and get approval from instructor before starting
- Must be different techique than your presentation!

X-ray absorption: Fermi's golden rule

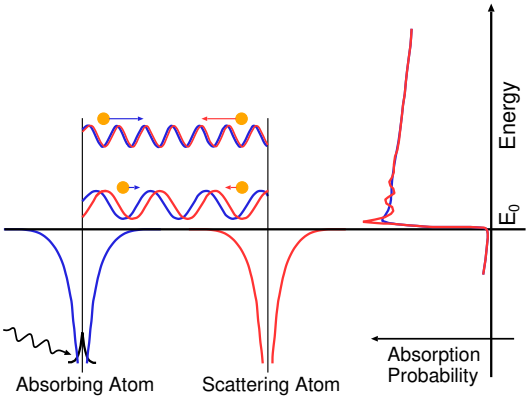

$$\mu(E) = \mu_0(E) + \Delta\mu(E)$$

X-ray absorption: Fermi's golden rule

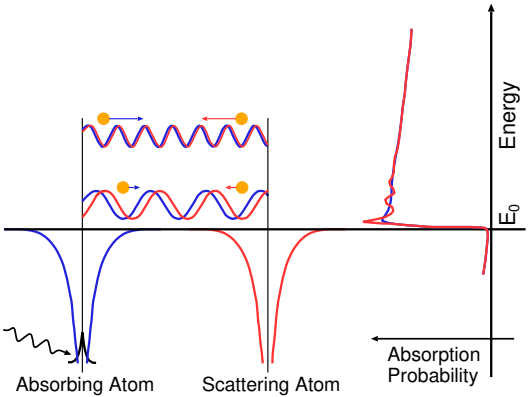

$$\mu(E) = \mu_0(E) + \Delta\mu(E) = \mu_0(E)[1 + \chi(E)]$$

X-ray absorption: Fermi's golden rule

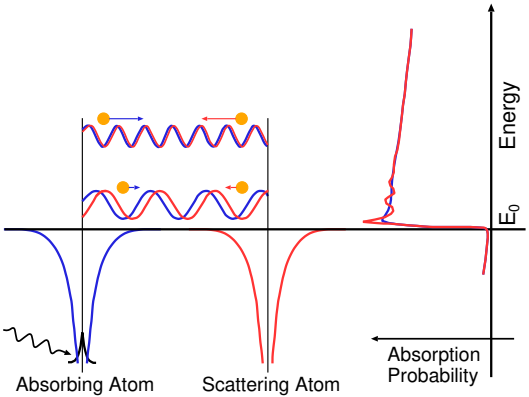

$$\mu(E) = \mu_0(E) + \Delta\mu(E) = \mu_0(E)[1 + \chi(E)]$$

$$\chi(k[E]) = \frac{\mu(E) - \mu_0(E)}{\mu_0(E)},$$

X-ray absorption: Fermi's golden rule

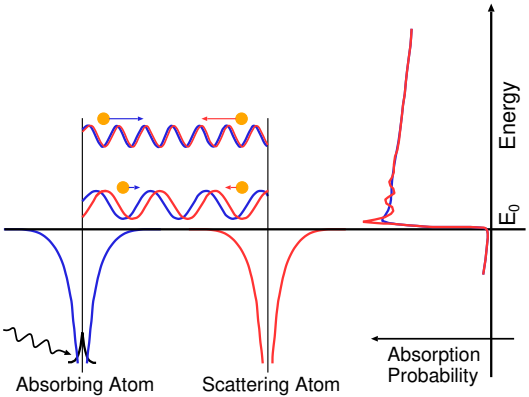

$$\mu(E) = \mu_0(E) + \Delta\mu(E) = \mu_0(E)[1 + \chi(E)]$$

$$\chi(k[E]) = \frac{\mu(E) - \mu_0(E)}{\mu_0(E)}, \quad k = \sqrt{\frac{2m(E - E_0)}{\hbar^2}}$$

X-ray absorption: Fermi's golden rule

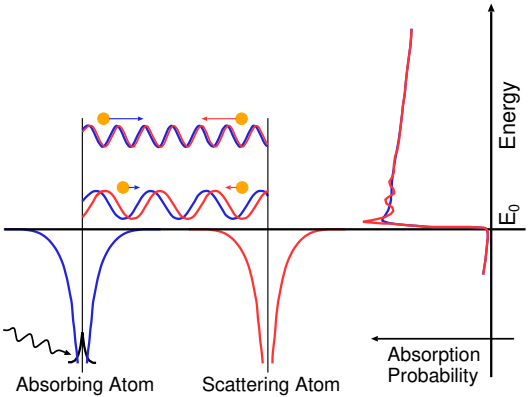

$$\mu(E) = \mu_0(E) + \Delta\mu(E) = \mu_0(E)[1 + \chi(E)]$$

$$\chi(k[E]) = \frac{\mu(E) - \mu_0(E)}{\mu_0(E)}, \quad k = \sqrt{\frac{2m(E - E_0)}{\hbar^2}}$$

$$\mu(E) \sim |\langle i|\mathcal{H}|f\rangle|^2$$

X-ray absorption: Fermi's golden rule

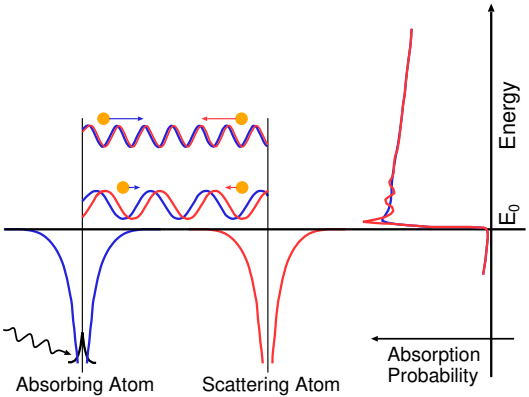

$$\mu(E) = \mu_0(E) + \Delta\mu(E) = \mu_0(E)[1 + \chi(E)]$$

$$\chi(k[E]) = \frac{\mu(E) - \mu_0(E)}{\mu_0(E)}, \quad k = \sqrt{\frac{2m(E - E_0)}{\hbar^2}}$$

$$\mu(E) \sim |\langle i|\mathcal{H}|f\rangle|^2$$

$\langle i|$ is the initial state which has a core level electron and the photon. This is not altered by the neighboring atom.

X-ray absorption: Fermi's golden rule

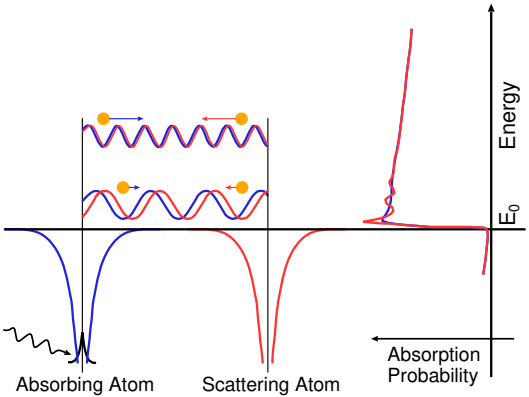

$$\mu(E) = \mu_0(E) + \Delta\mu(E) = \mu_0(E)[1 + \chi(E)]$$

$$\chi(k[E]) = \frac{\mu(E) - \mu_0(E)}{\mu_0(E)}, \quad k = \sqrt{\frac{2m(E - E_0)}{\hbar^2}}$$

$$\mu(E) \sim |\langle i|\mathcal{H}|f\rangle|^2$$

$\langle i|$ is the initial state which has a core level electron and the photon. This is not altered by the neighboring atom.

$\mathcal{H}$ is the interaction. In the dipole approximation, $\mathcal{H} = e^{ikr} \approx 1$.

X-ray absorption: Fermi's golden rule

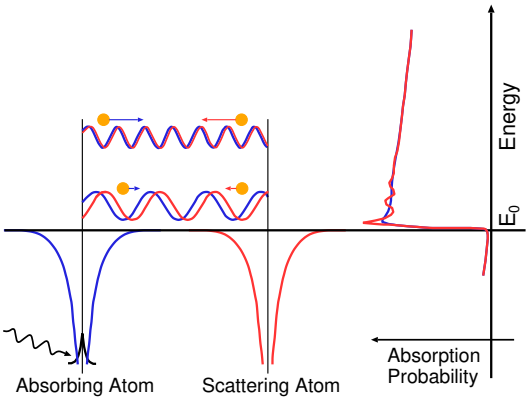

$$\mu(E) = \mu_0(E) + \Delta\mu(E) = \mu_0(E)[1 + \chi(E)]$$

$$\chi(k[E]) = \frac{\mu(E) - \mu_0(E)}{\mu_0(E)}, \quad k = \sqrt{\frac{2m(E - E_0)}{\hbar^2}}$$

$$\mu(E) \sim |\langle i|\mathcal{H}|f\rangle|^2$$

$\langle i|$ is the initial state which has a core level electron and the photon. This is not altered by the neighboring atom.

$\mathcal{H}$ is the interaction. In the dipole approximation, $\mathcal{H} = e^{ikr} \approx 1$.

$|f\rangle$ is the final state which has a photoelectron, a hole in the core, and no photon. This is altered by the neighboring atom: the photoelectron scatters.

μ and χ and the photoelectron wavefunction

Writing $|f\rangle = |f_0 + \Delta f\rangle$, where Δf gives the change in photoelectron final state due to backscattering from the neighboring atom, we can expand μ to get

μ and χ and the photoelectron wavefunction

Writing $|f\rangle = |f_0 + \Delta f\rangle$, where Δf gives the change in photoelectron final state due to backscattering from the neighboring atom, we can expand μ to get

$$\mu(E) \sim |\langle i|\mathcal{H}|f\rangle|^2$$

μ and χ and the photoelectron wavefunction

Writing $|f\rangle = |f_0 + \Delta f\rangle$, where Δf gives the change in photoelectron final state due to backscattering from the neighboring atom, we can expand μ to get

$$\mu(E) \sim |\langle i|\mathcal{H}|f\rangle|^2 = \langle i|\mathcal{H}|f_0 + \Delta f\rangle\langle f_0 + \Delta f|\mathcal{H}|i\rangle$$

μ and χ and the photoelectron wavefunction

Writing $|f\rangle = |f_0 + \Delta f\rangle$, where Δf gives the change in photoelectron final state due to backscattering from the neighboring atom, we can expand μ to get

$$\begin{aligned}\mu(E) &\sim |\langle i|\mathcal{H}|f\rangle|^2 = \langle i|\mathcal{H}|f_0 + \Delta f\rangle\langle f_0 + \Delta f|\mathcal{H}|i\rangle \\ &\approx \langle i|\mathcal{H}|f_0\rangle\langle f_0|\mathcal{H}|i\rangle\end{aligned}$$

μ and χ and the photoelectron wavefunction

Writing $|f\rangle = |f_0 + \Delta f\rangle$, where Δf gives the change in photoelectron final state due to backscattering from the neighboring atom, we can expand μ to get

$$\begin{aligned}\mu(E) &\sim |\langle i|\mathcal{H}|f\rangle|^2 = \langle i|\mathcal{H}|f_0 + \Delta f\rangle\langle f_0 + \Delta f|\mathcal{H}|i\rangle \\ &\approx \langle i|\mathcal{H}|f_0\rangle\langle f_0|\mathcal{H}|i\rangle + \langle i|\mathcal{H}|f_0\rangle\langle \Delta f|\mathcal{H}|i\rangle\end{aligned}$$

μ and χ and the photoelectron wavefunction

Writing $|f\rangle = |f_0 + \Delta f\rangle$, where Δf gives the change in photoelectron final state due to backscattering from the neighboring atom, we can expand μ to get

$$\begin{aligned}\mu(E) \sim |\langle i|\mathcal{H}|f\rangle|^2 &= \langle i|\mathcal{H}|f_0 + \Delta f\rangle\langle f_0 + \Delta f|\mathcal{H}|i\rangle \\ &\approx \langle i|\mathcal{H}|f_0\rangle\langle f_0|\mathcal{H}|i\rangle + \langle i|\mathcal{H}|f_0\rangle\langle \Delta f|\mathcal{H}|i\rangle + \langle i|\mathcal{H}|\Delta f\rangle\langle f_0|\mathcal{H}|i\rangle + \cdots\end{aligned}$$

μ and χ and the photoelectron wavefunction

Writing $|f\rangle = |f_0 + \Delta f\rangle$, where Δf gives the change in photoelectron final state due to backscattering from the neighboring atom, we can expand μ to get

$$\begin{aligned}
\mu(E) &\sim |\langle i|\mathcal{H}|f\rangle|^2 = \langle i|\mathcal{H}|f_0 + \Delta f\rangle\langle f_0 + \Delta f|\mathcal{H}|i\rangle \\
&\approx \langle i|\mathcal{H}|f_0\rangle\langle f_0|\mathcal{H}|i\rangle + \langle i|\mathcal{H}|f_0\rangle\langle \Delta f|\mathcal{H}|i\rangle + \langle i|\mathcal{H}|\Delta f\rangle\langle f_0|\mathcal{H}|i\rangle + \cdots \\
&= |\langle i|\mathcal{H}|f_0\rangle|^2 + \langle i|\mathcal{H}|f_0\rangle\langle \Delta f|\mathcal{H}|i\rangle + \langle i|\mathcal{H}|\Delta f\rangle\langle f_0|\mathcal{H}|i\rangle
\end{aligned}$$

μ and χ and the photoelectron wavefunction

Writing $|f\rangle = |f_0 + \Delta f\rangle$, where Δf gives the change in photoelectron final state due to backscattering from the neighboring atom, we can expand μ to get

$$\begin{aligned}
\mu(E) &\sim |\langle i|\mathcal{H}|f\rangle|^2 = \langle i|\mathcal{H}|f_0 + \Delta f\rangle\langle f_0 + \Delta f|\mathcal{H}|i\rangle \\
&\approx \langle i|\mathcal{H}|f_0\rangle\langle f_0|\mathcal{H}|i\rangle + \langle i|\mathcal{H}|f_0\rangle\langle \Delta f|\mathcal{H}|i\rangle + \langle i|\mathcal{H}|\Delta f\rangle\langle f_0|\mathcal{H}|i\rangle + \cdots \\
&= |\langle i|\mathcal{H}|f_0\rangle|^2 + \langle i|\mathcal{H}|f_0\rangle\langle \Delta f|\mathcal{H}|i\rangle + \langle i|\mathcal{H}|\Delta f\rangle\langle f_0|\mathcal{H}|i\rangle \\
&= |\langle i|\mathcal{H}|f_0\rangle|^2 \left[1 + \frac{\langle i|\mathcal{H}|f_0\rangle\langle \Delta f|\mathcal{H}|i\rangle}{|\langle i|\mathcal{H}|f_0\rangle|^2} + \frac{\langle i|\mathcal{H}|\Delta f\rangle\langle f_0|\mathcal{H}|i\rangle}{|\langle i|\mathcal{H}|f_0\rangle|^2}\right]
\end{aligned}$$

μ and χ and the photoelectron wavefunction

Writing $|f\rangle = |f_0 + \Delta f\rangle$, where Δf gives the change in photoelectron final state due to backscattering from the neighboring atom, we can expand μ to get

$$\begin{aligned}
\mu(E) &\sim |\langle i|\mathcal{H}|f\rangle|^2 = \langle i|\mathcal{H}|f_0 + \Delta f\rangle\langle f_0 + \Delta f|\mathcal{H}|i\rangle \\
&\approx \langle i|\mathcal{H}|f_0\rangle\langle f_0|\mathcal{H}|i\rangle + \langle i|\mathcal{H}|f_0\rangle\langle \Delta f|\mathcal{H}|i\rangle + \langle i|\mathcal{H}|\Delta f\rangle\langle f_0|\mathcal{H}|i\rangle + \cdots \\
&= |\langle i|\mathcal{H}|f_0\rangle|^2 + \langle i|\mathcal{H}|f_0\rangle\langle \Delta f|\mathcal{H}|i\rangle + \langle i|\mathcal{H}|\Delta f\rangle\langle f_0|\mathcal{H}|i\rangle \\
&= |\langle i|\mathcal{H}|f_0\rangle|^2 \left[1 + \frac{\langle i|\mathcal{H}|f_0\rangle\langle \Delta f|\mathcal{H}|i\rangle}{|\langle i|\mathcal{H}|f_0\rangle|^2} + \frac{\langle i|\mathcal{H}|\Delta f\rangle\langle f_0|\mathcal{H}|i\rangle}{|\langle i|\mathcal{H}|f_0\rangle|^2}\right]
\end{aligned}$$

Compare this to $\mu(E) = \mu_0(E)[1 + \chi(E)]$ and we see that

μ and χ and the photoelectron wavefunction

Writing $|f\rangle = |f_0 + \Delta f\rangle$, where Δf gives the change in photoelectron final state due to backscattering from the neighboring atom, we can expand μ to get

$$\begin{aligned}
\mu(E) &\sim |\langle i|\mathcal{H}|f\rangle|^2 = \langle i|\mathcal{H}|f_0 + \Delta f\rangle\langle f_0 + \Delta f|\mathcal{H}|i\rangle \\
&\approx \langle i|\mathcal{H}|f_0\rangle\langle f_0|\mathcal{H}|i\rangle + \langle i|\mathcal{H}|f_0\rangle\langle \Delta f|\mathcal{H}|i\rangle + \langle i|\mathcal{H}|\Delta f\rangle\langle f_0|\mathcal{H}|i\rangle + \cdots \\
&= |\langle i|\mathcal{H}|f_0\rangle|^2 + \langle i|\mathcal{H}|f_0\rangle\langle \Delta f|\mathcal{H}|i\rangle + \langle i|\mathcal{H}|\Delta f\rangle\langle f_0|\mathcal{H}|i\rangle \\
&= |\langle i|\mathcal{H}|f_0\rangle|^2 \left[1 + \frac{\langle i|\mathcal{H}|f_0\rangle\langle \Delta f|\mathcal{H}|i\rangle}{|\langle i|\mathcal{H}|f_0\rangle|^2} + \frac{\langle i|\mathcal{H}|\Delta f\rangle\langle f_0|\mathcal{H}|i\rangle}{|\langle i|\mathcal{H}|f_0\rangle|^2}\right]
\end{aligned}$$

Compare this to $\mu(E) = \mu_0(E)[1 + \chi(E)]$ and we see that

$$\mu_0(E) \sim |\langle i|\mathcal{H}|f_0\rangle|^2 \qquad \text{atomic background}$$

μ and χ and the photoelectron wavefunction

Writing $|f\rangle = |f_0 + \Delta f\rangle$, where Δf gives the change in photoelectron final state due to backscattering from the neighboring atom, we can expand μ to get

$$\begin{aligned}
\mu(E) &\sim |\langle i|\mathcal{H}|f\rangle|^2 = \langle i|\mathcal{H}|f_0 + \Delta f\rangle\langle f_0 + \Delta f|\mathcal{H}|i\rangle \\
&\approx \langle i|\mathcal{H}|f_0\rangle\langle f_0|\mathcal{H}|i\rangle + \langle i|\mathcal{H}|f_0\rangle\langle \Delta f|\mathcal{H}|i\rangle + \langle i|\mathcal{H}|\Delta f\rangle\langle f_0|\mathcal{H}|i\rangle + \cdots \\
&= |\langle i|\mathcal{H}|f_0\rangle|^2 + \langle i|\mathcal{H}|f_0\rangle\langle \Delta f|\mathcal{H}|i\rangle + \langle i|\mathcal{H}|\Delta f\rangle\langle f_0|\mathcal{H}|i\rangle \\
&= |\langle i|\mathcal{H}|f_0\rangle|^2 \left[1 + \frac{\langle i|\mathcal{H}|f_0\rangle\langle \Delta f|\mathcal{H}|i\rangle}{|\langle i|\mathcal{H}|f_0\rangle|^2} + \frac{\langle i|\mathcal{H}|\Delta f\rangle\langle f_0|\mathcal{H}|i\rangle}{|\langle i|\mathcal{H}|f_0\rangle|^2}\right]
\end{aligned}$$

Compare this to $\mu(E) = \mu_0(E)[1 + \chi(E)]$ and we see that

$$\mu_0(E) \sim |\langle i|\mathcal{H}|f_0\rangle|^2 \qquad \text{atomic background}$$

$$\chi(E) \sim \langle i|\mathcal{H}|\Delta f\rangle \qquad \text{XAFS oscillations}$$

μ and χ and the photoelectron wavefunction

Writing $|f\rangle = |f_0 + \Delta f\rangle$, where Δf gives the change in photoelectron final state due to backscattering from the neighboring atom, we can expand μ to get

$$\begin{aligned}
\mu(E) &\sim |\langle i|\mathcal{H}|f\rangle|^2 = \langle i|\mathcal{H}|f_0 + \Delta f\rangle\langle f_0 + \Delta f|\mathcal{H}|i\rangle \\
&\approx \langle i|\mathcal{H}|f_0\rangle\langle f_0|\mathcal{H}|i\rangle + \langle i|\mathcal{H}|f_0\rangle\langle \Delta f|\mathcal{H}|i\rangle + \langle i|\mathcal{H}|\Delta f\rangle\langle f_0|\mathcal{H}|i\rangle + \cdots \\
&= |\langle i|\mathcal{H}|f_0\rangle|^2 + \langle i|\mathcal{H}|f_0\rangle\langle \Delta f|\mathcal{H}|i\rangle + \langle i|\mathcal{H}|\Delta f\rangle\langle f_0|\mathcal{H}|i\rangle \\
&= |\langle i|\mathcal{H}|f_0\rangle|^2 \left[1 + \frac{\langle i|\mathcal{H}|f_0\rangle\langle \Delta f|\mathcal{H}|i\rangle}{|\langle i|\mathcal{H}|f_0\rangle|^2} + \frac{\langle i|\mathcal{H}|\Delta f\rangle\langle f_0|\mathcal{H}|i\rangle}{|\langle i|\mathcal{H}|f_0\rangle|^2}\right]
\end{aligned}$$

Compare this to $\mu(E) = \mu_0(E)[1 + \chi(E)]$ and we see that

$$\mu_0(E) \sim |\langle i|\mathcal{H}|f_0\rangle|^2 \qquad \text{atomic background}$$
$$\chi(E) \sim \langle i|\mathcal{H}|\Delta f\rangle \sim \langle i|\Delta f\rangle \qquad \text{XAFS oscillations}$$

μ and χ and the photoelectron wavefunction

Writing $|f\rangle = |f_0 + \Delta f\rangle$, where Δf gives the change in photoelectron final state due to backscattering from the neighboring atom, we can expand μ to get

$$\begin{aligned}
\mu(E) &\sim |\langle i|\mathcal{H}|f\rangle|^2 = \langle i|\mathcal{H}|f_0 + \Delta f\rangle\langle f_0 + \Delta f|\mathcal{H}|i\rangle \\
&\approx \langle i|\mathcal{H}|f_0\rangle\langle f_0|\mathcal{H}|i\rangle + \langle i|\mathcal{H}|f_0\rangle\langle \Delta f|\mathcal{H}|i\rangle + \langle i|\mathcal{H}|\Delta f\rangle\langle f_0|\mathcal{H}|i\rangle + \cdots \\
&= |\langle i|\mathcal{H}|f_0\rangle|^2 + \langle i|\mathcal{H}|f_0\rangle\langle \Delta f|\mathcal{H}|i\rangle + \langle i|\mathcal{H}|\Delta f\rangle\langle f_0|\mathcal{H}|i\rangle \\
&= |\langle i|\mathcal{H}|f_0\rangle|^2 \left[1 + \frac{\langle i|\mathcal{H}|f_0\rangle\langle \Delta f|\mathcal{H}|i\rangle}{|\langle i|\mathcal{H}|f_0\rangle|^2} + \frac{\langle i|\mathcal{H}|\Delta f\rangle\langle f_0|\mathcal{H}|i\rangle}{|\langle i|\mathcal{H}|f_0\rangle|^2}\right]
\end{aligned}$$

Compare this to $\mu(E) = \mu_0(E)[1 + \chi(E)]$ and we see that

$$\begin{aligned}
\mu_0(E) &\sim |\langle i|\mathcal{H}|f_0\rangle|^2 && \text{atomic background} \\
\chi(E) &\sim \langle i|\mathcal{H}|\Delta f\rangle \sim \langle i|\Delta f\rangle && \text{XAFS oscillations}
\end{aligned}$$

$$\chi(E) \sim \langle i|\Delta f\rangle$$

μ and χ and the photoelectron wavefunction

Writing $|f\rangle = |f_0 + \Delta f\rangle$, where Δf gives the change in photoelectron final state due to backscattering from the neighboring atom, we can expand μ to get

$$\begin{aligned}
\mu(E) &\sim |\langle i|\mathcal{H}|f\rangle|^2 = \langle i|\mathcal{H}|f_0 + \Delta f\rangle\langle f_0 + \Delta f|\mathcal{H}|i\rangle \\
&\approx \langle i|\mathcal{H}|f_0\rangle\langle f_0|\mathcal{H}|i\rangle + \langle i|\mathcal{H}|f_0\rangle\langle \Delta f|\mathcal{H}|i\rangle + \langle i|\mathcal{H}|\Delta f\rangle\langle f_0|\mathcal{H}|i\rangle + \cdots \\
&= |\langle i|\mathcal{H}|f_0\rangle|^2 + \langle i|\mathcal{H}|f_0\rangle\langle \Delta f|\mathcal{H}|i\rangle + \langle i|\mathcal{H}|\Delta f\rangle\langle f_0|\mathcal{H}|i\rangle \\
&= |\langle i|\mathcal{H}|f_0\rangle|^2 \left[1 + \frac{\langle i|\mathcal{H}|f_0\rangle\langle \Delta f|\mathcal{H}|i\rangle}{|\langle i|\mathcal{H}|f_0\rangle|^2} + \frac{\langle i|\mathcal{H}|\Delta f\rangle\langle f_0|\mathcal{H}|i\rangle}{|\langle i|\mathcal{H}|f_0\rangle|^2}\right]
\end{aligned}$$

Compare this to $\mu(E) = \mu_0(E)[1 + \chi(E)]$ and we see that

$$\mu_0(E) \sim |\langle i|\mathcal{H}|f_0\rangle|^2 \qquad \text{atomic background}$$

$$\chi(E) \sim \langle i|\mathcal{H}|\Delta f\rangle \sim \langle i|\Delta f\rangle \qquad \text{XAFS oscillations}$$

$$\chi(E) \sim \langle i|\Delta f\rangle \sim \int \psi_{core}\psi_{\mathrm{scatt}}(r)\, dr$$

μ and χ and the photoelectron wavefunction

Writing $|f\rangle = |f_0 + \Delta f\rangle$, where Δf gives the change in photoelectron final state due to backscattering from the neighboring atom, we can expand μ to get

$$\begin{aligned}
\mu(E) &\sim |\langle i|\mathcal{H}|f\rangle|^2 = \langle i|\mathcal{H}|f_0 + \Delta f\rangle\langle f_0 + \Delta f|\mathcal{H}|i\rangle \\
&\approx \langle i|\mathcal{H}|f_0\rangle\langle f_0|\mathcal{H}|i\rangle + \langle i|\mathcal{H}|f_0\rangle\langle \Delta f|\mathcal{H}|i\rangle + \langle i|\mathcal{H}|\Delta f\rangle\langle f_0|\mathcal{H}|i\rangle + \cdots \\
&= |\langle i|\mathcal{H}|f_0\rangle|^2 + \langle i|\mathcal{H}|f_0\rangle\langle \Delta f|\mathcal{H}|i\rangle + \langle i|\mathcal{H}|\Delta f\rangle\langle f_0|\mathcal{H}|i\rangle \\
&= |\langle i|\mathcal{H}|f_0\rangle|^2 \left[1 + \frac{\langle i|\mathcal{H}|f_0\rangle\langle \Delta f|\mathcal{H}|i\rangle}{|\langle i|\mathcal{H}|f_0\rangle|^2} + \frac{\langle i|\mathcal{H}|\Delta f\rangle\langle f_0|\mathcal{H}|i\rangle}{|\langle i|\mathcal{H}|f_0\rangle|^2}\right]
\end{aligned}$$

Compare this to $\mu(E) = \mu_0(E)[1 + \chi(E)]$ and we see that

$$\mu_0(E) \sim |\langle i|\mathcal{H}|f_0\rangle|^2 \qquad \text{atomic background}$$

$$\chi(E) \sim \langle i|\mathcal{H}|\Delta f\rangle \sim \langle i|\Delta f\rangle \qquad \text{XAFS oscillations}$$

$$\chi(E) \sim \langle i|\Delta f\rangle \sim \int \psi_{core}\psi_{\mathrm{scatt}}(r)\, dr \sim \int \delta(r)\psi_{\mathrm{scatt}}(r)\, dr$$

μ and χ and the photoelectron wavefunction

Writing $|f\rangle = |f_0 + \Delta f\rangle$, where Δf gives the change in photoelectron final state due to backscattering from the neighboring atom, we can expand μ to get

$$\begin{aligned}
\mu(E) &\sim |\langle i|\mathcal{H}|f\rangle|^2 = \langle i|\mathcal{H}|f_0 + \Delta f\rangle\langle f_0 + \Delta f|\mathcal{H}|i\rangle \\
&\approx \langle i|\mathcal{H}|f_0\rangle\langle f_0|\mathcal{H}|i\rangle + \langle i|\mathcal{H}|f_0\rangle\langle \Delta f|\mathcal{H}|i\rangle + \langle i|\mathcal{H}|\Delta f\rangle\langle f_0|\mathcal{H}|i\rangle + \cdots \\
&= |\langle i|\mathcal{H}|f_0\rangle|^2 + \langle i|\mathcal{H}|f_0\rangle\langle \Delta f|\mathcal{H}|i\rangle + \langle i|\mathcal{H}|\Delta f\rangle\langle f_0|\mathcal{H}|i\rangle \\
&= |\langle i|\mathcal{H}|f_0\rangle|^2 \left[1 + \frac{\langle i|\mathcal{H}|f_0\rangle\langle \Delta f|\mathcal{H}|i\rangle}{|\langle i|\mathcal{H}|f_0\rangle|^2} + \frac{\langle i|\mathcal{H}|\Delta f\rangle\langle f_0|\mathcal{H}|i\rangle}{|\langle i|\mathcal{H}|f_0\rangle|^2}\right]
\end{aligned}$$

Compare this to $\mu(E) = \mu_0(E)[1 + \chi(E)]$ and we see that

$$\mu_0(E) \sim |\langle i|\mathcal{H}|f_0\rangle|^2 \qquad \text{atomic background}$$

$$\chi(E) \sim \langle i|\mathcal{H}|\Delta f\rangle \sim \langle i|\Delta f\rangle \qquad \text{XAFS oscillations}$$

$$\chi(E) \sim \langle i|\Delta f\rangle \sim \int \psi_{core}\psi_{\mathrm{scatt}}(r)\, dr \sim \int \delta(r)\psi_{\mathrm{scatt}}(r)\, dr = \psi_{\mathrm{scatt}}(0)$$

Computing the scattered wavefunction

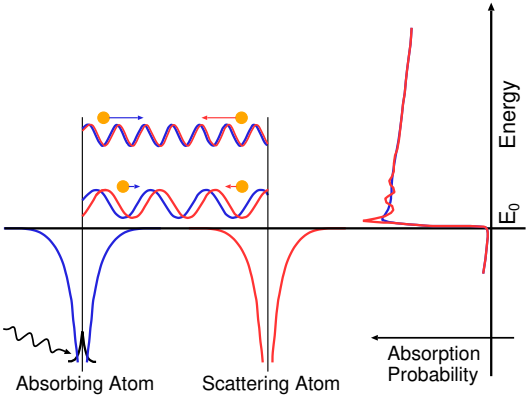

Assume that emitted photoelectron is a spherical wave

Computing the scattered wavefunction

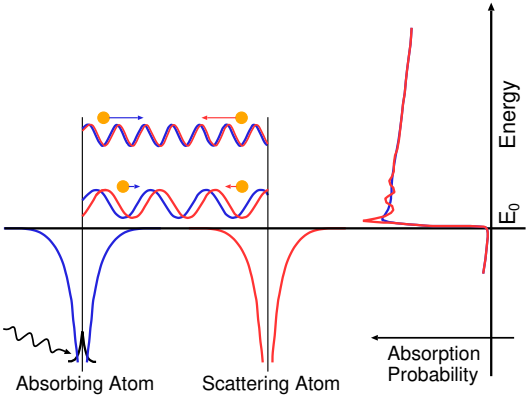

Assume that emitted photoelectron is a spherical wave

$$\psi(k,r) = \frac{e^{ikr}}{kr}$$

Computing the scattered wavefunction

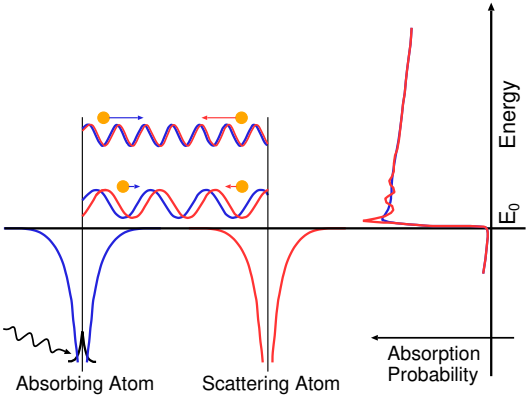

Assume that emitted photoelectron is a spherical wave

$$\psi(k, r) = \frac{e^{ikr}}{kr}$$

follow the electron as it:

Computing the scattered wavefunction

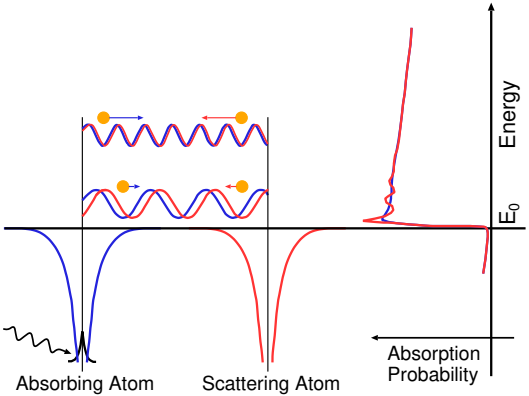

$$\chi(k) \sim \psi_{scatt}(0) = \frac{e^{ikR}}{kR}$$

Assume that emitted photoelectron is a spherical wave

$$\psi(k, r) = \frac{e^{ikr}}{kr}$$

follow the electron as it:

a. leaves the absorbing atom

Computing the scattered wavefunction

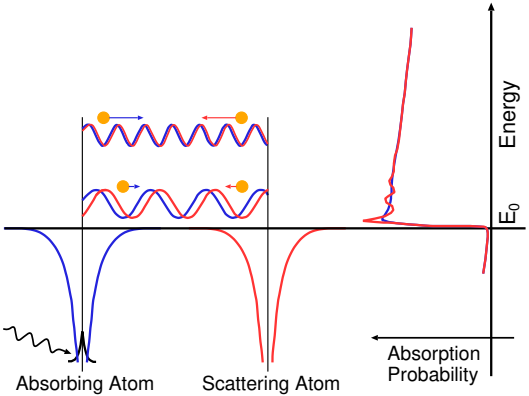

Assume that emitted photoelectron is a spherical wave

$$\psi(k,r) = \frac{e^{ikr}}{kr}$$

follow the electron as it:

a. leaves the absorbing atom

b. scatters from the neighbor atom

$$\chi(k) \sim \psi_{scatt}(0) = \frac{e^{ikR}}{kR}[2kf(k)e^{i\delta(k)}]$$

Computing the scattered wavefunction

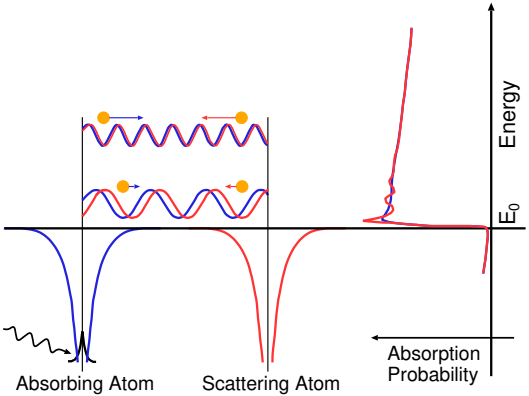

Assume that emitted photoelectron is a spherical wave

$$\psi(k,r) = \frac{e^{ikr}}{kr}$$

follow the electron as it:

a. leaves the absorbing atom

b. scatters from the neighbor atom

c. returns to the absorbing atom

$$\chi(k) \sim \psi_{scatt}(0) = \frac{e^{ikR}}{kR}[2kf(k)e^{i\delta(k)}]\frac{e^{ikR}}{kR}$$

Computing the scattered wavefunction

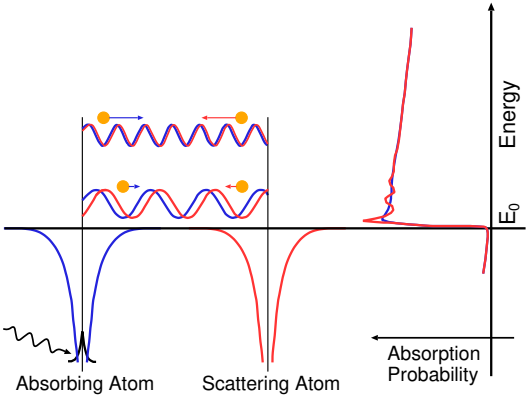

Assume that emitted photoelectron is a spherical wave

$$\psi(k,r) = \frac{e^{ikr}}{kr}$$

follow the electron as it:

a. leaves the absorbing atom

b. scatters from the neighbor atom

c. returns to the absorbing atom

$$\chi(k) \sim \psi_{scatt}(0) = \frac{e^{ikR}}{kR}[2kf(k)e^{i\delta(k)}]\frac{e^{ikR}}{kR}$$

where scattering from the neighboring atom gives the amplitude $f(k)$ and phase-shift $\delta(k)$ to the photoelectron

Computing the scattered wavefunction

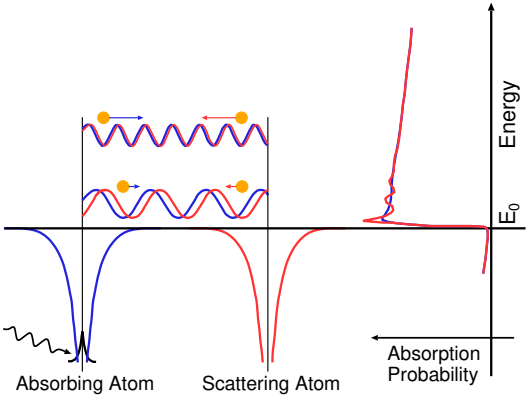

Assume that emitted photoelectron is a spherical wave

$$\psi(k,r) = \frac{e^{ikr}}{kr}$$

follow the electron as it:

a. leaves the absorbing atom

b. scatters from the neighbor atom

c. returns to the absorbing atom

$$\chi(k) \sim \psi_{scatt}(0) = \frac{e^{ikR}}{kR}[2kf(k)e^{i\delta(k)}]\frac{e^{ikR}}{kR} = \frac{2e^{i(2kR+\delta(k))}}{kR^2}f(k)$$

where scattering from the neighboring atom gives the amplitude $f(k)$ and phase-shift $\delta(k)$ to the photoelectron

Development of the EXAFS equation

Including the complex conjugate,

Development of the EXAFS equation

Including the complex conjugate,

$$\chi(k) \sim \frac{2f(k)}{kR^2}\left[e^{i(2kR+\delta(k))} + e^{-i(2kR+\delta(k))}\right]$$

Development of the EXAFS equation

Including the complex conjugate, and simplifying

$$\chi(k) \sim \frac{2f(k)}{kR^2}\left[e^{i(2kR+\delta(k))} + e^{-i(2kR+\delta(k))}\right] = \frac{f(k)}{kR^2}\cos\left[2kR + \delta(k)\right]$$

Development of the EXAFS equation

Including the complex conjugate, and simplifying

$$\chi(k) \sim \frac{2f(k)}{kR^2}\left[e^{i(2kR+\delta(k))} + e^{-i(2kR+\delta(k))}\right] = \frac{f(k)}{kR^2}\cos\left[2kR + \delta(k)\right]$$

incorporating an additional $\pi/2$ phase shift, we have the EXAFS equation for one scattering atom

Development of the EXAFS equation

Including the complex conjugate, and simplifying

$$\chi(k) \sim \frac{2f(k)}{kR^2}\left[e^{i(2kR+\delta(k))} + e^{-i(2kR+\delta(k))}\right] = \frac{f(k)}{kR^2}\cos\left[2kR+\delta(k)\right]$$

incorporating an additional $\pi/2$ phase shift, we have the EXAFS equation for one scattering atom

$$\chi(k) = \frac{f(k)}{kR^2}\sin\left[2kR+\delta(k)\right]$$

Development of the EXAFS equation

Including the complex conjugate, and simplifying

$$\chi(k) \sim \frac{2f(k)}{kR^2}\left[e^{i(2kR+\delta(k))} + e^{-i(2kR+\delta(k))}\right] = \frac{f(k)}{kR^2}\cos\left[2kR+\delta(k)\right]$$

incorporating an additional $\pi/2$ phase shift, we have the EXAFS equation for one scattering atom

$$\chi(k) = \frac{f(k)}{kR^2}\sin\left[2kR+\delta(k)\right]$$

for N neighboring atoms, and with thermal and static disorder of σ^2 giving the mean-square disorder in R, we have

Development of the EXAFS equation

Including the complex conjugate, and simplifying

$$\chi(k) \sim \frac{2f(k)}{kR^2}\left[e^{i(2kR+\delta(k))} + e^{-i(2kR+\delta(k))}\right] = \frac{f(k)}{kR^2}\cos\left[2kR+\delta(k)\right]$$

incorporating an additional $\pi/2$ phase shift, we have the EXAFS equation for one scattering atom

$$\chi(k) = \frac{f(k)}{kR^2}\sin\left[2kR+\delta(k)\right] \quad \longrightarrow \quad \chi(k) = \frac{Nf(k)e^{-2k^2\sigma^2}}{kR^2}\sin\left[2kR+\delta(k)\right]$$

for N neighboring atoms, and with thermal and static disorder of σ^2 giving the mean-square disorder in R, we have

Development of the EXAFS equation

Including the complex conjugate, and simplifying

$$\chi(k) \sim \frac{2f(k)}{kR^2}\left[e^{i(2kR+\delta(k))} + e^{-i(2kR+\delta(k))}\right] = \frac{f(k)}{kR^2}\cos\left[2kR+\delta(k)\right]$$

incorporating an additional $\pi/2$ phase shift, we have the EXAFS equation for one scattering atom

$$\chi(k) = \frac{f(k)}{kR^2}\sin\left[2kR+\delta(k)\right] \quad \longrightarrow \quad \chi(k) = \frac{Nf(k)e^{-2k^2\sigma^2}}{kR^2}\sin\left[2kR+\delta(k)\right]$$

for N neighboring atoms, and with thermal and static disorder of σ^2 giving the mean-square disorder in R, we have

a real system has atoms at different distances and of different types so all these contributions are summed to get a better version of the EXAFS equation:

Development of the EXAFS equation

Including the complex conjugate, and simplifying

$$\chi(k) \sim \frac{2f(k)}{kR^2}\left[e^{i(2kR+\delta(k))} + e^{-i(2kR+\delta(k))}\right] = \frac{f(k)}{kR^2}\cos\left[2kR+\delta(k)\right]$$

incorporating an additional $\pi/2$ phase shift, we have the EXAFS equation for one scattering atom

$$\chi(k) = \frac{f(k)}{kR^2}\sin\left[2kR+\delta(k)\right] \quad \longrightarrow \quad \chi(k) = \frac{Nf(k)e^{-2k^2\sigma^2}}{kR^2}\sin\left[2kR+\delta(k)\right]$$

for N neighboring atoms, and with thermal and static disorder of σ^2 giving the mean-square disorder in R, we have

a real system has atoms at different distances and of different types so all these contributions are summed to get a better version of the EXAFS equation:

$$\chi(k) = \sum_j \frac{N_j f_j(k) e^{-2k^2\sigma_j^2}}{kR_j{}^2}\sin[2kR_j + \delta_j(k)]$$

Scattering amplitude and phase shift: $f(k)$ and $\delta(k)$

The scattering amplitude $f(k)$ and phase-shift $\delta(k)$ depend on atomic number

Scattering amplitude and phase shift: $f(k)$ and $\delta(k)$

The scattering amplitude $f(k)$ and phase-shift $\delta(k)$ depend on atomic number

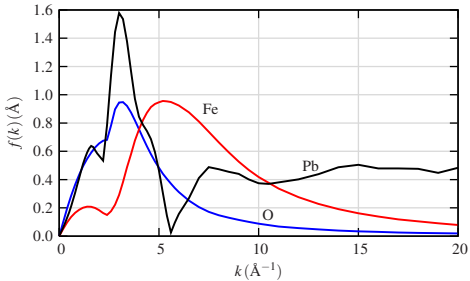

Scattering amplitude and phase shift: $f(k)$ and $\delta(k)$

The scattering amplitude $f(k)$ and phase-shift $\delta(k)$ depend on atomic number

The scattering amplitude $f(k)$ peaks at different k values and extends to higher-k for heavier elements. For very heavy elements, there is structure in $f(k)$

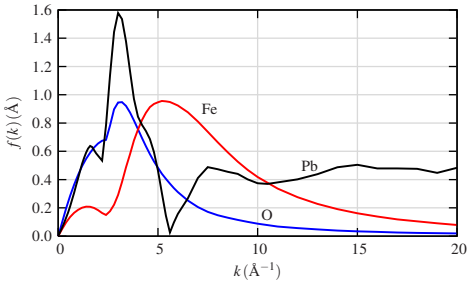

Scattering amplitude and phase shift: $f(k)$ and $\delta(k)$

The scattering amplitude $f(k)$ and phase-shift $\delta(k)$ depend on atomic number

The scattering amplitude $f(k)$ peaks at different k values and extends to higher-k for heavier elements. For very heavy elements, there is structure in $f(k)$

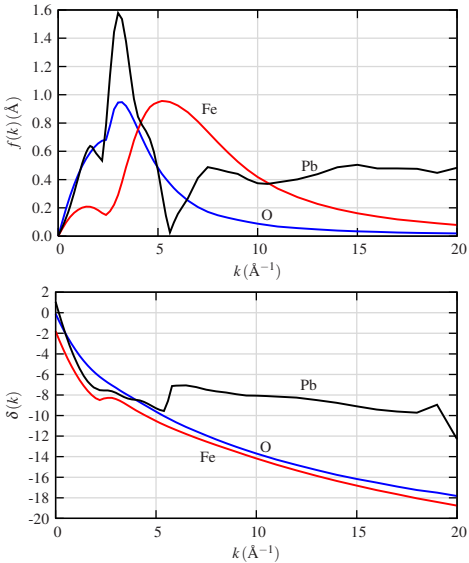

Scattering amplitude and phase shift: $f(k)$ and $\delta(k)$

The scattering amplitude $f(k)$ and phase-shift $\delta(k)$ depend on atomic number

The scattering amplitude $f(k)$ peaks at different k values and extends to higher-k for heavier elements. For very heavy elements, there is structure in $f(k)$

The phase shift $\delta(k)$ shows sharp changes for very heavy elements

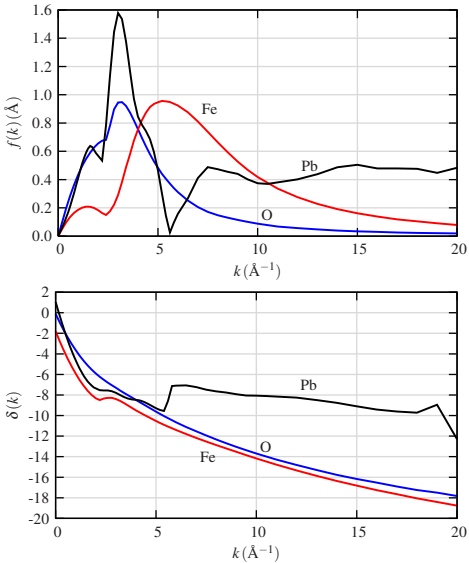

Scattering amplitude and phase shift: $f(k)$ and $\delta(k)$

The scattering amplitude $f(k)$ and phase-shift $\delta(k)$ depend on atomic number

The scattering amplitude $f(k)$ peaks at different k values and extends to higher-k for heavier elements. For very heavy elements, there is structure in $f(k)$

The phase shift $\delta(k)$ shows sharp changes for very heavy elements

These functions can be calculated accurately (say with the program FEFF) for modeling EXAFS

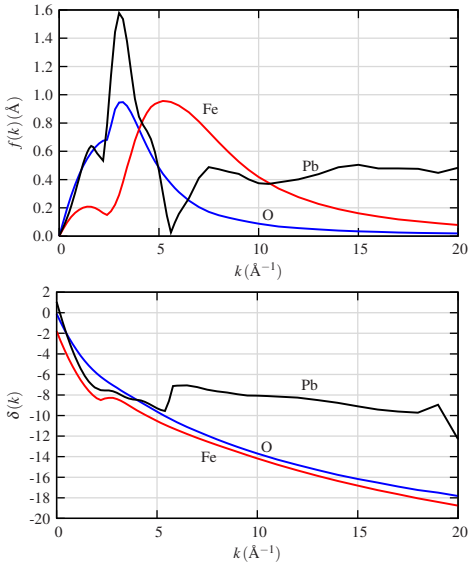

Scattering amplitude and phase shift: $f(k)$ and $\delta(k)$

The scattering amplitude $f(k)$ and phase-shift $\delta(k)$ depend on atomic number

The scattering amplitude $f(k)$ peaks at different k values and extends to higher-k for heavier elements. For very heavy elements, there is structure in $f(k)$

The phase shift $\delta(k)$ shows sharp changes for very heavy elements

These functions can be calculated accurately (say with the program FEFF) for modeling EXAFS

Z can usually be determined to ± 5. Fe and O can be distinguished, but Fe and Mn cannot be

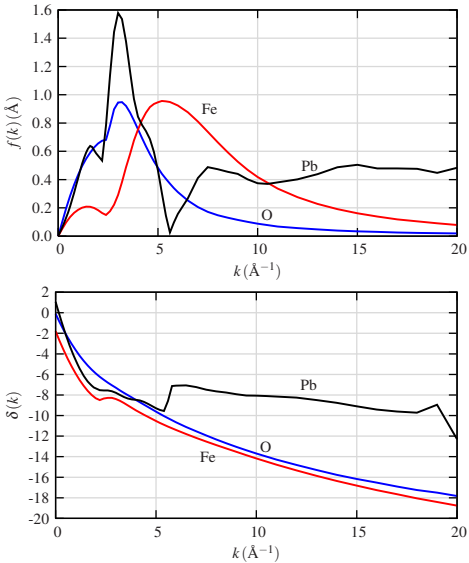

The EXAFS equation: What we left out

This simple description is qualitatively right, but for quantitative EXAFS calculations, it's important to consider these points:

The EXAFS equation: What we left out

This simple description is qualitatively right, but for quantitative EXAFS calculations, it's important to consider these points:

Inelastic Losses The photoelectron mean-free path, including self-energy and finite lifetime of the core-hole.

The EXAFS equation: What we left out

This simple description is qualitatively right, but for quantitative EXAFS calculations, it's important to consider these points:

Inelastic Losses The photoelectron mean-free path, including self-energy and finite lifetime of the core-hole.

multiple scattering the photoelectron can scatter from multiple atoms. Most important at low k, and leads to a path expansion.

The EXAFS equation: What we left out

This simple description is qualitatively right, but for quantitative EXAFS calculations, it's important to consider these points:

Inelastic Losses The photoelectron mean-free path, including self-energy and finite lifetime of the core-hole.

multiple scattering the photoelectron can scatter from multiple atoms. Most important at low k, and leads to a path expansion.

Muffin-Tin Approximation: The scattering calculation needs a real-space potential, and a muffin-tin approximation is most tractable.

The EXAFS equation: What we left out

This simple description is qualitatively right, but for quantitative EXAFS calculations, it's important to consider these points:

Inelastic Losses The photoelectron mean-free path, including self-energy and finite lifetime of the core-hole.

multiple scattering the photoelectron can scatter from multiple atoms. Most important at low k, and leads to a path expansion.

Muffin-Tin Approximation: The scattering calculation needs a real-space potential, and a muffin-tin approximation is most tractable.

Polarization Effects synchrotron beams are highly polarized, which needs to be taken into account. This is simple for K-edges ($s \rightarrow p$ is dipole), and less so for L-edges (where both $p \rightarrow d$ and $p \rightarrow s$ contribute).

The EXAFS equation: What we left out

This simple description is qualitatively right, but for quantitative EXAFS calculations, it's important to consider these points:

Inelastic Losses The photoelectron mean-free path, including self-energy and finite lifetime of the core-hole.

multiple scattering the photoelectron can scatter from multiple atoms. Most important at low k, and leads to a path expansion.

Muffin-Tin Approximation: The scattering calculation needs a real-space potential, and a muffin-tin approximation is most tractable.

Polarization Effects synchrotron beams are highly polarized, which needs to be taken into account. This is simple for K-edges ($s \rightarrow p$ is dipole), and less so for L-edges (where both $p \rightarrow d$ and $p \rightarrow s$ contribute).

Disorder Terms thermal and static disorder in real systems should be properly considered: A topic of its own.

The EXAFS equation: What we left out

This simple description is qualitatively right, but for quantitative EXAFS calculations, it's important to consider these points:

Inelastic Losses The photoelectron mean-free path, including self-energy and finite lifetime of the core-hole.

multiple scattering the photoelectron can scatter from multiple atoms. Most important at low k, and leads to a path expansion.

Muffin-Tin Approximation: The scattering calculation needs a real-space potential, and a muffin-tin approximation is most tractable.

Polarization Effects synchrotron beams are highly polarized, which needs to be taken into account. This is simple for K-edges ($s \rightarrow p$ is dipole), and less so for L-edges (where both $p \rightarrow d$ and $p \rightarrow s$ contribute).

Disorder Terms thermal and static disorder in real systems should be properly considered: A topic of its own.

Generally, the calculations (FEFF, etc) include these effects. We'll discuss of few of these in more detail ...

The photoelectron mean-free path

$$\chi(k) = \sum_j \frac{N_j f_j(k) e^{-2k^2\sigma_j^2}}{k {R_j}^2} \sin[2kR_j + \delta_j(k)]$$

The photoelectron mean-free path

$$\chi(k) = \sum_j \frac{N_j f_j(k) e^{-2k^2\sigma_j^2}}{k{R_j}^2} \sin[2kR_j + \delta_j(k)]$$

The EXAFS equation was obtained by approximating the photoelectron wavefunction by a spherical wave, $\psi(k, r) \sim e^{ikr}/kr$

The photoelectron mean-free path

$$\chi(k) = \sum_j \frac{N_j f_j(k) e^{-2k^2\sigma_j^2}}{k{R_j}^2} \sin[2kR_j + \delta_j(k)]$$

The EXAFS equation was obtained by approximating the photoelectron wavefunction by a spherical wave, $\psi(k, r) \sim e^{ikr}/kr$

But the interference that gives rise to EXAFS requires that the wavefunction retain coherence and inelastic scattering and the finite lifetime of the core-hole can destroy that coherence

The photoelectron mean-free path

$$\chi(k) = \sum_j \frac{N_j f_j(k) e^{-2k^2\sigma_j^2}}{k{R_j}^2} \sin[2kR_j + \delta_j(k)]$$

The EXAFS equation was obtained by approximating the photoelectron wavefunction by a spherical wave, $\psi(k, r) \sim e^{ikr}/kr$

But the interference that gives rise to EXAFS requires that the wavefunction retain coherence and inelastic scattering and the finite lifetime of the core-hole can destroy that coherence

Using a damped wavefunction instead

The photoelectron mean-free path

$$\chi(k) = \sum_j \frac{N_j f_j(k) e^{-2k^2\sigma_j^2}}{k{R_j}^2} \sin[2kR_j + \delta_j(k)]$$

The EXAFS equation was obtained by approximating the photoelectron wavefunction by a spherical wave, $\psi(k, r) \sim e^{ikr}/kr$

But the interference that gives rise to EXAFS requires that the wavefunction retain coherence and inelastic scattering and the finite lifetime of the core-hole can destroy that coherence

Using a damped wavefunction instead $\psi(k, r) \sim \frac{e^{ikr} e^{-r/\lambda(k)}}{kr}$

The photoelectron mean-free path

$$\chi(k) = \sum_j \frac{N_j f_j(k) e^{-2k^2\sigma_j^2}}{k{R_j}^2} \sin[2kR_j + \delta_j(k)]$$

The EXAFS equation was obtained by approximating the photoelectron wavefunction by a spherical wave, $\psi(k, r) \sim e^{ikr}/kr$

But the interference that gives rise to EXAFS requires that the wavefunction retain coherence and inelastic scattering and the finite lifetime of the core-hole can destroy that coherence

Using a damped wavefunction instead $\psi(k, r) \sim \frac{e^{ikr} e^{-r/\lambda(k)}}{kr}$

where $\lambda(k)$ is the photoelectron's mean free path (including core-hole lifetime), the EXAFS equation becomes:

The photoelectron mean-free path

$$\chi(k) = \sum_j \frac{N_j f_j(k) e^{-2k^2\sigma_j^2}}{kR_j^2} \sin[2kR_j + \delta_j(k)]$$

The EXAFS equation was obtained by approximating the photoelectron wavefunction by a spherical wave, $\psi(k, r) \sim e^{ikr}/kr$

But the interference that gives rise to EXAFS requires that the wavefunction retain coherence and inelastic scattering and the finite lifetime of the core-hole can destroy that coherence

Using a damped wavefunction instead $\psi(k, r) \sim \frac{e^{ikr} e^{-r/\lambda(k)}}{kr}$

where $\lambda(k)$ is the photoelectron's mean free path (including core-hole lifetime), the EXAFS equation becomes:

$$\chi(k) = \sum_j \frac{N_j f_j(k) e^{-2R_j/\lambda(k)} e^{-2k^2\sigma_j^2}}{kR_j^2} \sin[2kR_j + \delta_j(k)]$$

The photoelectron mean-free path

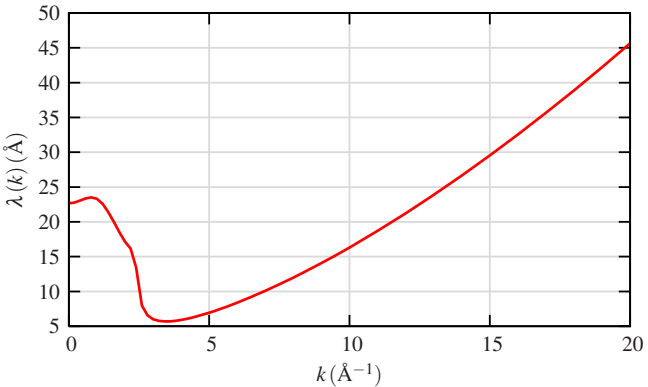

The photoelectron mean-free path

λ is mostly independent of the system, but depends strongly on k:

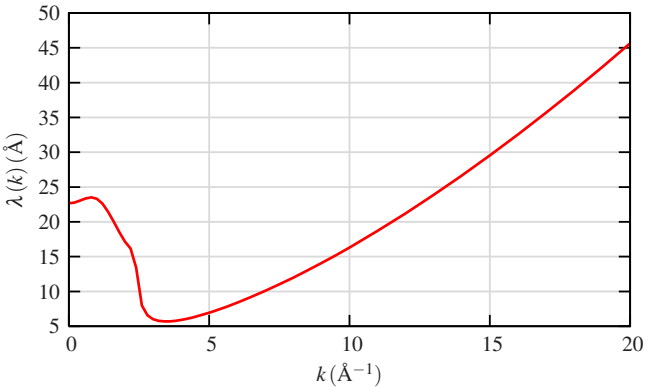

The photoelectron mean-free path

λ is mostly independent of the system, but depends strongly on k:

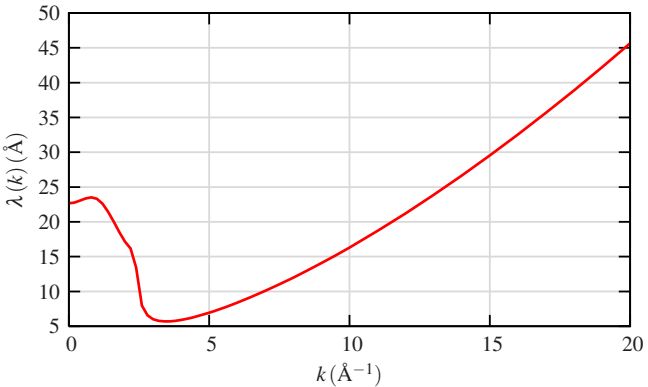

for $3\,\text{Å}^{-1} < k < 15\,\text{Å}^{-1}$,
$\lambda < 30\,\text{Å}$

The photoelectron mean-free path

λ is mostly independent of the system, but depends strongly on k:

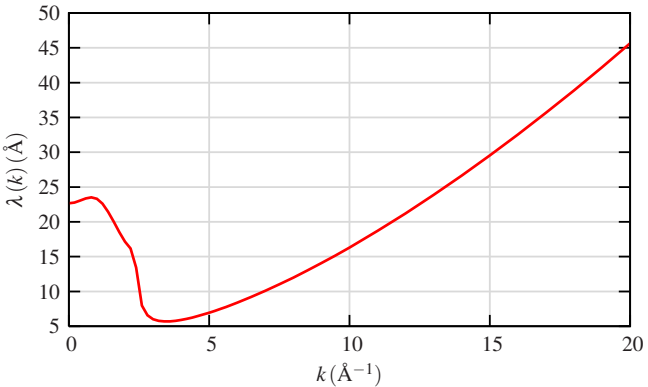

for $3\,\text{Å}^{-1} < k < 15\,\text{Å}^{-1}$,
$\lambda < 30\,\text{Å}$

along with the R^{-2} term this makes EXAFS a local atomic probe

The photoelectron mean-free path

λ is mostly independent of the system, but depends strongly on k:

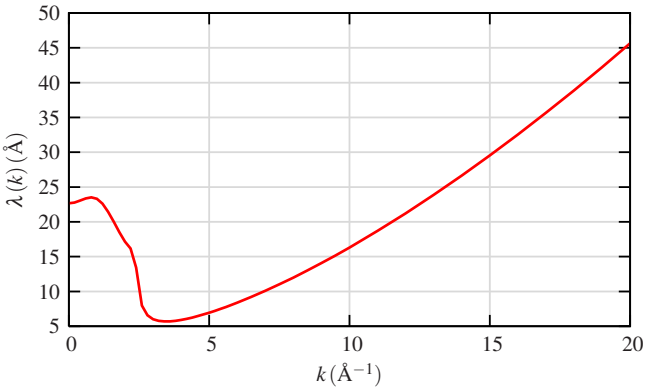

for $3\,\text{Å}^{-1} < \text{k} < 15\,\text{Å}^{-1}$,
$\lambda < 30\,\text{Å}$

along with the R^{-2} term this makes EXAFS a local atomic probe

for XANES ($k < 3\,\text{Å}^{-1}$), both λ and R^{-2} become large: making XANES not really a local probe

S_0^2: Amplitude reduction term

Another important amplitude reduction term is due to the relaxation of the other electrons in the absorbing atom to the hole in the core level:

S_0^2: Amplitude reduction term

Another important amplitude reduction term is due to the relaxation of the other electrons in the absorbing atom to the hole in the core level:

$$S_0^2 = |\langle \Phi_f^{N-1} | \Phi_0^{N-1} \rangle|^2$$

S_0^2: Amplitude reduction term

Another important amplitude reduction term is due to the relaxation of the other electrons in the absorbing atom to the hole in the core level:

$$S_0^2 = |\langle \Phi_f^{N-1} | \Phi_0^{N-1} \rangle|^2$$

$|\Phi_0^{N-1}\rangle = (N-1)$ – electrons in unexcited atom

S_0^2: Amplitude reduction term

Another important amplitude reduction term is due to the relaxation of the other electrons in the absorbing atom to the hole in the core level:

$$S_0^2 = |\langle \Phi_f^{N-1} | \Phi_0^{N-1} \rangle|^2$$

$|\Phi_0^{N-1}\rangle = (N-1)$ – electrons in unexcited atom

$\langle \Phi_f^{N-1}| = (N-1)$ – electrons, relaxed by core-hole

S_0^2: Amplitude reduction term

Another important amplitude reduction term is due to the relaxation of the other electrons in the absorbing atom to the hole in the core level:

$$S_0^2 = |\langle \Phi_f^{N-1} | \Phi_0^{N-1} \rangle|^2$$

$|\Phi_0^{N-1}\rangle = (N-1)$ – electrons in unexcited atom

$\langle \Phi_f^{N-1}| = (N-1)$ – electrons, relaxed by core-hole

S_0^2 is usually taken as a constant:

$$0.7 < S_0^2 < 1.0$$

S_0^2: Amplitude reduction term

Another important amplitude reduction term is due to the relaxation of the other electrons in the absorbing atom to the hole in the core level:

$$S_0^2 = |\langle \Phi_f^{N-1} | \Phi_0^{N-1} \rangle|^2$$

$|\Phi_0^{N-1}\rangle = (N-1)$ – electrons in unexcited atom

$\langle \Phi_f^{N-1}| = (N-1)$ – electrons, relaxed by core-hole

S_0^2 is usually taken as a constant:

$$0.7 < S_0^2 < 1.0$$

and is used as a fitting parameter that multiplies χ:

S_0^2: Amplitude reduction term

Another important amplitude reduction term is due to the relaxation of the other electrons in the absorbing atom to the hole in the core level:

$$S_0^2 = |\langle \Phi_f^{N-1} | \Phi_0^{N-1} \rangle|^2$$

$|\Phi_0^{N-1}\rangle = (N-1)$ – electrons in unexcited atom

$\langle \Phi_f^{N-1}| = (N-1)$ – electrons, relaxed by core-hole

S_0^2 is usually taken as a constant:

$$0.7 < S_0^2 < 1.0$$

and is used as a fitting parameter that multiplies χ:

S_0^2 is completely correlated with N (!!!)

S_0^2: Amplitude reduction term

Another important amplitude reduction term is due to the relaxation of the other electrons in the absorbing atom to the hole in the core level:

$$S_0^2 = |\langle \Phi_f^{N-1} | \Phi_0^{N-1} \rangle|^2$$

$|\Phi_0^{N-1}\rangle = (N-1)$ – electrons in unexcited atom

$\langle \Phi_f^{N-1}| = (N-1)$ – electrons, relaxed by core-hole

S_0^2 is usually taken as a constant:

$$0.7 < S_0^2 < 1.0$$

and is used as a fitting parameter that multiplies χ:

S_0^2 is completely correlated with N (!!!)

This, and other experimental and theoretical issues, make EXAFS amplitudes (and therefore N) less precise than EXAFS phases (and therefore R)

The EXAFS equation

The full EXAFS equation can be used to model and interpret experimental data

The EXAFS equation

The full EXAFS equation can be used to model and interpret experimental data

$$\chi(k) = \sum_j \frac{N_j S_0^2 f_j(k) e^{-2R_j/\lambda(k)}\, e^{-2k^2\sigma_j^2}}{kR_j^2} \sin\left[2kR_j + \delta_j(k)\right]$$

The EXAFS equation

The full EXAFS equation can be used to model and interpret experimental data

$$\chi(k) = \sum_j \frac{N_j S_0^2 f_j(k) e^{-2R_j/\lambda(k)}\, e^{-2k^2\sigma_j^2}}{kR_j^2} \sin\left[2kR_j + \delta_j(k)\right]$$

where the sum can be either over shells of atoms (Fe-O, Fe-Fe) or ...

The EXAFS equation

The full EXAFS equation can be used to model and interpret experimental data

$$\chi(k) = \sum_j \frac{N_j S_0^2 f_j(k) e^{-2R_j/\lambda(k)}\, e^{-2k^2\sigma_j^2}}{kR_j^2} \sin\left[2kR_j + \delta_j(k)\right]$$

where the sum can be either over shells of atoms (Fe-O, Fe-Fe) or ...
... over possible scattering paths (preferred) of the photoelectron.

The EXAFS equation

The full EXAFS equation can be used to model and interpret experimental data

$$\chi(k) = \sum_j \frac{N_j S_0^2 f_j(k) e^{-2R_j/\lambda(k)}\, e^{-2k^2\sigma_j^2}}{kR_j^2} \sin\left[2kR_j + \delta_j(k)\right]$$

where the sum can be either over shells of atoms (Fe-O, Fe-Fe) or ...
... over possible scattering paths (preferred) of the photoelectron.

N_j: path degeneracy

The EXAFS equation

The full EXAFS equation can be used to model and interpret experimental data

$$\chi(k) = \sum_j \frac{N_j S_0^2 f_j(k) e^{-2R_j/\lambda(k)}\, e^{-2k^2\sigma_j^2}}{kR_j^2} \sin\left[2kR_j + \delta_j(k)\right]$$

where the sum can be either over shells of atoms (Fe-O, Fe-Fe) or ...
... over possible scattering paths (preferred) of the photoelectron.

N_j: path degeneracy

R_j: half path length

The EXAFS equation

The full EXAFS equation can be used to model and interpret experimental data

$$\chi(k) = \sum_j \frac{N_j S_0^2 f_j(k) e^{-2R_j/\lambda(k)}\, e^{-2k^2\sigma_j^2}}{kR_j^2} \sin\left[2kR_j + \delta_j(k)\right]$$

where the sum can be either over shells of atoms (Fe-O, Fe-Fe) or ...
... over possible scattering paths (preferred) of the photoelectron.

- N_j: path degeneracy
- R_j: half path length
- σ_j^2: path "disorder"

The EXAFS equation

The full EXAFS equation can be used to model and interpret experimental data

$$\chi(k) = \sum_j \frac{N_j S_0^2 f_j(k) e^{-2R_j/\lambda(k)}\, e^{-2k^2\sigma_j^2}}{k R_j^2} \sin\left[2kR_j + \delta_j(k)\right]$$

where the sum can be either over shells of atoms (Fe-O, Fe-Fe) or ...
... over possible scattering paths (preferred) of the photoelectron.

- N_j: path degeneracy
- R_j: half path length
- σ_j^2: path "disorder"
- S_0^2: amplitude reduction factor

The EXAFS equation

The full EXAFS equation can be used to model and interpret experimental data

$$\chi(k) = \sum_j \frac{N_j S_0^2 f_j(k) e^{-2R_j/\lambda(k)}\, e^{-2k^2\sigma_j^2}}{kR_j^2} \sin\left[2kR_j + \delta_j(k)\right]$$

where the sum can be either over shells of atoms (Fe-O, Fe-Fe) or ...
... over possible scattering paths (preferred) of the photoelectron.

N_j: path degeneracy

R_j: half path length

σ_j^2: path "disorder"

S_0^2: amplitude reduction factor

k is the photoelectron wave number

The EXAFS equation

The full EXAFS equation can be used to model and interpret experimental data

$$\chi(k) = \sum_j \frac{N_j S_0^2 f_j(k) e^{-2R_j/\lambda(k)}\, e^{-2k^2\sigma_j^2}}{kR_j^2} \sin\left[2kR_j + \delta_j(k)\right]$$

where the sum can be either over shells of atoms (Fe-O, Fe-Fe) or ...
... over possible scattering paths (preferred) of the photoelectron.

- N_j: path degeneracy
- R_j: half path length
- σ_j^2: path "disorder"
- S_0^2: amplitude reduction factor

k is the photoelectron wave number

$f_j(k)$: scattering factor for the path

The EXAFS equation

The full EXAFS equation can be used to model and interpret experimental data

$$\chi(k) = \sum_j \frac{N_j S_0^2 f_j(k) e^{-2R_j/\lambda(k)}\, e^{-2k^2\sigma_j^2}}{kR_j^2} \sin\left[2kR_j + \delta_j(k)\right]$$

where the sum can be either over shells of atoms (Fe-O, Fe-Fe) or ...
... over possible scattering paths (preferred) of the photoelectron.

- N_j: path degeneracy
- R_j: half path length
- σ_j^2: path "disorder"
- S_0^2: amplitude reduction factor

k is the photoelectron wave number

- $f_j(k)$: scattering factor for the path
- $\delta_j(k)$: phase shift for the path

The EXAFS equation

The full EXAFS equation can be used to model and interpret experimental data

$$\chi(k) = \sum_j \frac{N_j S_0^2 f_j(k) e^{-2R_j/\lambda(k)}\, e^{-2k^2\sigma_j^2}}{kR_j^2} \sin\left[2kR_j + \delta_j(k)\right]$$

where the sum can be either over shells of atoms (Fe-O, Fe-Fe) or ...
... over possible scattering paths (preferred) of the photoelectron.

- N_j: path degeneracy
- R_j: half path length
- σ_j^2: path "disorder"
- S_0^2: amplitude reduction factor

k is the photoelectron wave number

- $f_j(k)$: scattering factor for the path
- $\delta_j(k)$: phase shift for the path
- $\lambda(k)$: photoelectron mean free path

The EXAFS equation

The full EXAFS equation can be used to model and interpret experimental data

$$\chi(k) = \sum_j \frac{N_j S_0^2 f_j(k) e^{-2R_j/\lambda(k)}\, e^{-2k^2\sigma_j^2}}{kR_j^2} \sin\left[2kR_j + \delta_j(k)\right]$$

where the sum can be either over shells of atoms (Fe-O, Fe-Fe) or ...
... over possible scattering paths (preferred) of the photoelectron.

- N_j: path degeneracy
- R_j: half path length
- σ_j^2: path "disorder"
- S_0^2: amplitude reduction factor
- k is the photoelectron wave number
- $f_j(k)$: scattering factor for the path
- $\delta_j(k)$: phase shift for the path
- $\lambda(k)$: photoelectron mean free path

Because we can compute $f(k)$ and $\delta(k)$, and $\lambda(k)$ we can determine Z, R, N, and σ^2 for scattering paths to neighboring atoms by fitting the data.

Sum over paths and multiple scattering

A sum over scattering paths allows multiple-scattering paths: the photoelectron scatters from more than one atom before returning to the absorbing atom:

Sum over paths and multiple scattering

A sum over scattering paths allows multiple-scattering paths: the photoelectron scatters from more than one atom before returning to the absorbing atom:

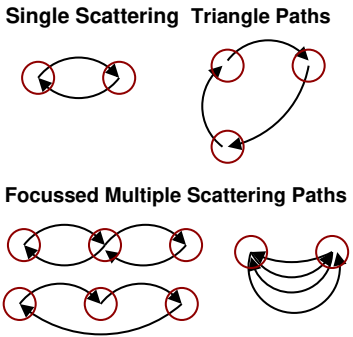

Sum over paths and multiple scattering

A sum over scattering paths allows multiple-scattering paths: the photoelectron scatters from more than one atom before returning to the absorbing atom:

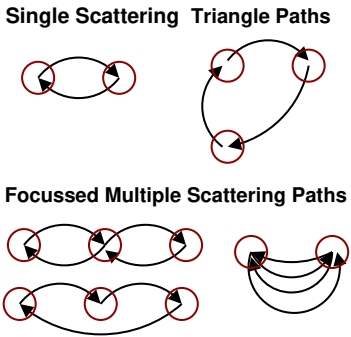

For multi-bounce paths, the total amplitude depends on the angles in the photoelectron path

Sum over paths and multiple scattering

A sum over scattering paths allows multiple-scattering paths: the photoelectron scatters from more than one atom before returning to the absorbing atom:

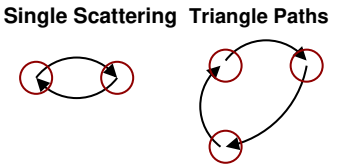

For multi-bounce paths, the total amplitude depends on the angles in the photoelectron path

Triangle Paths with angles $45^\circ < \theta < 135^\circ$ aren't strong, but there can be a lot of them

Sum over paths and multiple scattering

A sum over scattering paths allows multiple-scattering paths: the photoelectron scatters from more than one atom before returning to the absorbing atom:

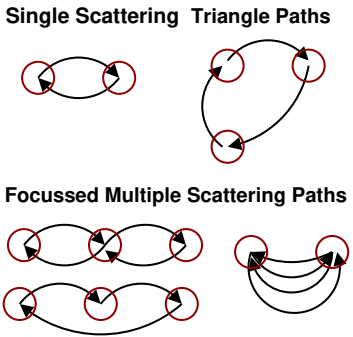

For multi-bounce paths, the total amplitude depends on the angles in the photoelectron path

Triangle Paths with angles $45^\circ < \theta < 135^\circ$ aren't strong, but there can be a lot of them

Linear paths, with angles $\theta \approx 180^\circ$, are very strong: the photoelectron can be focused through one atom to the next

Sum over paths and multiple scattering

A sum over scattering paths allows multiple-scattering paths: the photoelectron scatters from more than one atom before returning to the absorbing atom:

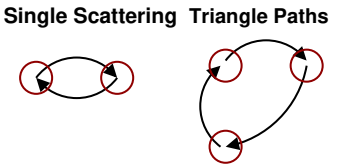

For multi-bounce paths, the total amplitude depends on the angles in the photoelectron path

Triangle Paths with angles $45^\circ < \theta < 135^\circ$ aren't strong, but there can be a lot of them

Linear paths, with angles $\theta \approx 180^\circ$, are very strong: the photoelectron can be focused through one atom to the next

FEFF calculates these effects and includes them in $f(k)$ and $\delta(k)$ for the EXAFS equation so that all paths look the same in the analysis

Multiple Scattering is strongest when $\theta > 150^\circ$ and the strong angular dependence can be used to measure bond angles

Sum over paths and multiple scattering

A sum over scattering paths allows multiple-scattering paths: the photoelectron scatters from more than one atom before returning to the absorbing atom:

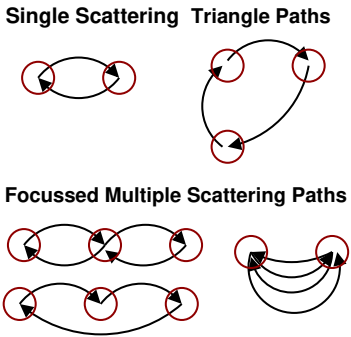

For multi-bounce paths, the total amplitude depends on the angles in the photoelectron path

Triangle Paths with angles $45^\circ < \theta < 135^\circ$ aren't strong, but there can be a lot of them

Linear paths, with angles $\theta \approx 180^\circ$, are very strong: the photoelectron can be focused through one atom to the next

FEFF calculates these effects and includes them in $f(k)$ and $\delta(k)$ for the EXAFS equation so that all paths look the same in the analysis

Multiple Scattering is strongest when $\theta > 150^\circ$ and the strong angular dependence can be used to measure bond angles

For first shell analysis, multiple scattering is hardly ever needed

Sn_4P_3/graphite composite anode

Sn_4P_3 synthesized by high energy ball milling, then ball milled again with graphite to obtain composite

"In situ EXAFS-derived mechanism of highly reversible tin phosphide/graphite composite anode for Li-ion batteries," Y. Ding, Z. Li, E.V. Timofeeva, and C.U. Segre, *Adv. Energy Mater.* **8**, 1702134 (2018).

Sn_4P_3/graphite composite anode

Sn_4P_3 synthesized by high energy ball milling, then ball milled again with graphite to obtain composite

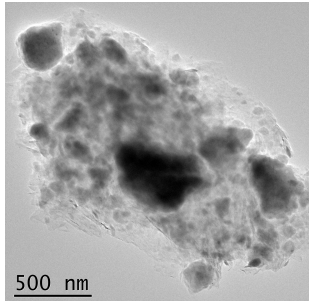

"In situ EXAFS-derived mechanism of highly reversible tin phosphide/graphite composite anode for Li-ion batteries," Y. Ding, Z. Li, E.V. Timofeeva, and C.U. Segre, *Adv. Energy Mater.* **8**, 1702134 (2018).

Sn_4P_3/graphite composite anode

Sn_4P_3 synthesized by high energy ball milling, then ball milled again with graphite to obtain composite

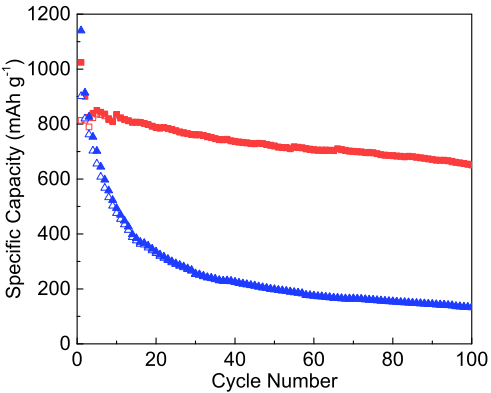

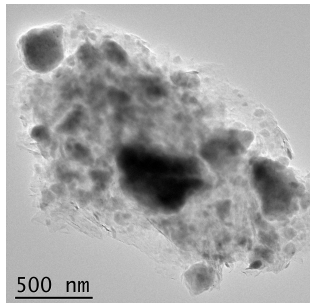

"In situ EXAFS-derived mechanism of highly reversible tin phosphide/graphite composite anode for Li-ion batteries," Y. Ding, Z. Li, E.V. Timofeeva, and C.U. Segre, *Adv. Energy Mater.* **8**, 1702134 (2018).

Sn_4P_3/graphite composite anode

Sn_4P_3 synthesized by high energy ball milling, then ball milled again with graphite to obtain composite

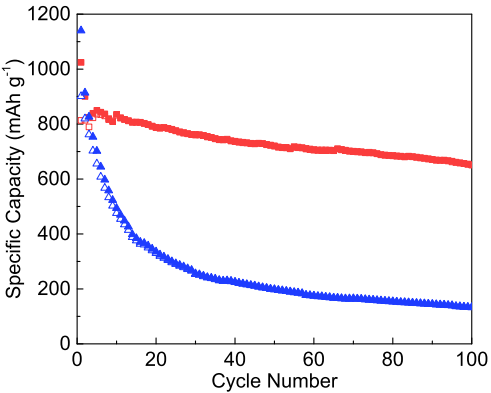

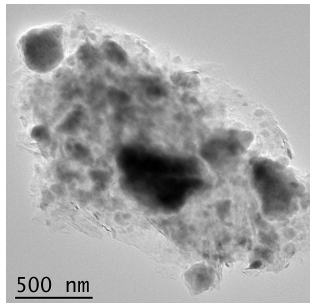

Sn_4P_3/graphite composite shows stable, reversible capacity of 610 mAh/g for 100 cycles at C/2 compared to rapidly fading pure Sn_4P_3 material.

"In situ EXAFS-derived mechanism of highly reversible tin phosphide/graphite composite anode for Li-ion batteries," Y. Ding, Z. Li, E.V. Timofeeva, and C.U. Segre, *Adv. Energy Mater.* **8**, 1702134 (2018).

In situ EXAFS of Sn_4P_3/graphite

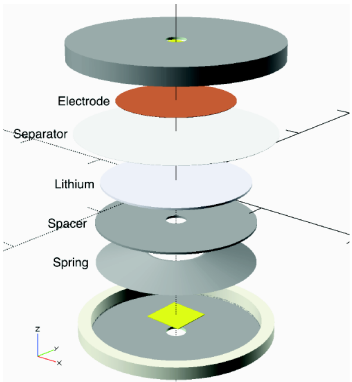

"In situ EXAFS-derived mechanism of highly reversible tin phosphide/graphite composite anode for Li-ion batteries," Y. Ding, Z. Li, E.V. Timofeeva, and C.U. Segre, *Adv. Energy Mater.* **8**, 1702134 (2018).

In situ EXAFS of Sn_4P_3/graphite

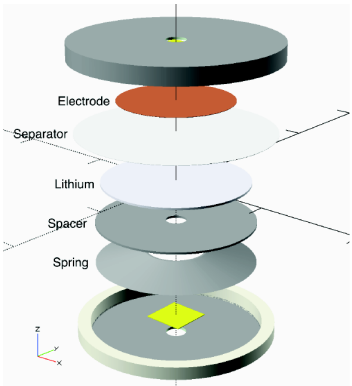

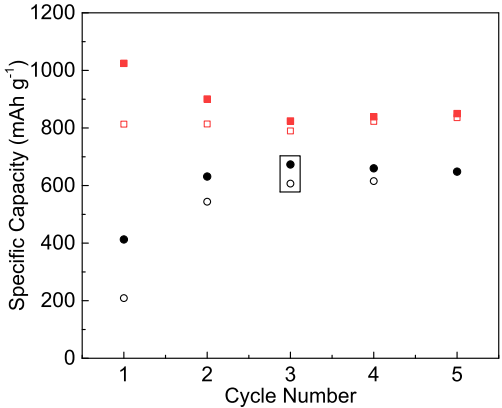

"In situ EXAFS-derived mechanism of highly reversible tin phosphide/graphite composite anode for Li-ion batteries," Y. Ding, Z. Li, E.V. Timofeeva, and C.U. Segre, *Adv. Energy Mater.* **8**, 1702134 (2018).

In situ EXAFS of Sn_4P_3/graphite

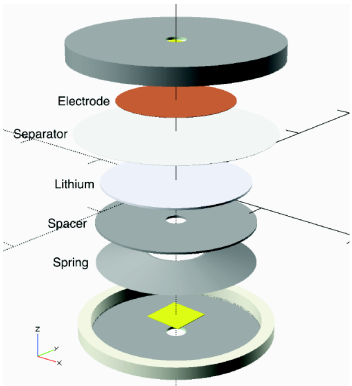

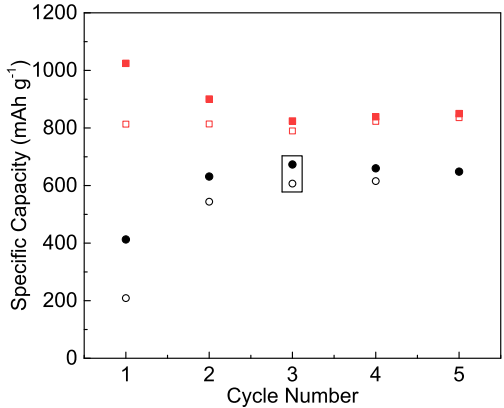

Results for *in situ* coin cell are close to the capacity of the unmodified cell at C/4, indicating good reversibility by the 3^{rd} cycle.

"In situ EXAFS-derived mechanism of highly reversible tin phosphide/graphite composite anode for Li-ion batteries," Y. Ding, Z. Li, E.V. Timofeeva, and C.U. Segre, *Adv. Energy Mater.* **8**, 1702134 (2018).

Third cycle comparison

By the third lithiation and third delithiation, the difference between pure Sn_4P_3 and the Sn_4P_3/graphite composite is clear.

"In situ EXAFS-derived mechanism of highly reversible tin phosphide/graphite composite anode for Li-ion batteries," Y. Ding, Z. Li, E.V. Timofeeva, and C.U. Segre, *Adv. Energy Mater.* **8**, 1702134 (2018).

Third cycle comparison

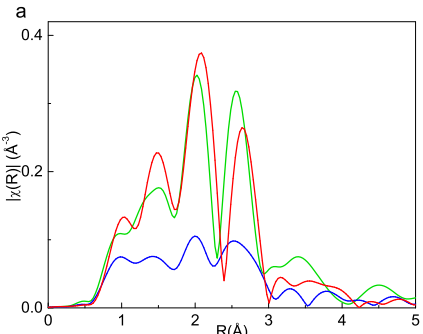

Sn_4P_3/graphite composite

By the third lithiation and third delithiation, the difference between pure Sn_4P_3 and the Sn_4P_3/graphite composite is clear.

"In situ EXAFS-derived mechanism of highly reversible tin phosphide/graphite composite anode for Li-ion batteries," Y. Ding, Z. Li, E.V. Timofeeva, and C.U. Segre, *Adv. Energy Mater.* **8**, 1702134 (2018).

Third cycle comparison

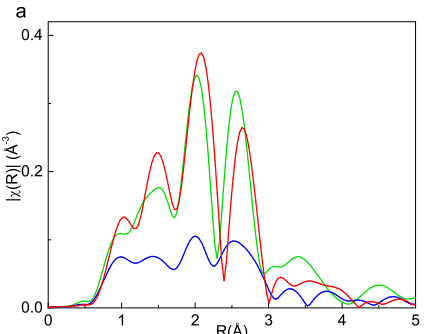

Sn_4P_3/graphite composite

By the third lithiation and third delithiation, the difference between pure Sn_4P_3 and the Sn_4P_3/graphite composite is clear.

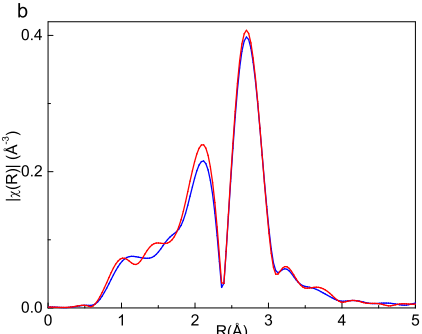

pure Sn_4P_3

"In situ EXAFS-derived mechanism of highly reversible tin phosphide/graphite composite anode for Li-ion batteries," Y. Ding, Z. Li, E.V. Timofeeva, and C.U. Segre, *Adv. Energy Mater.* **8**, 1702134 (2018).

Third cycle comparison

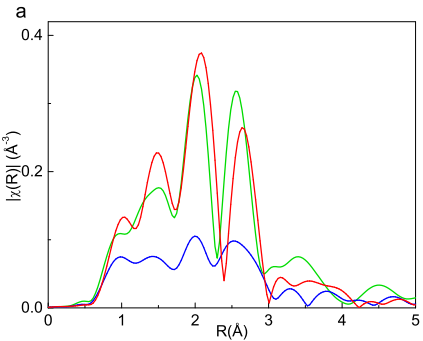

Sn_4P_3/graphite composite

By the third lithiation and third delithiation, the difference between pure Sn_4P_3 and the Sn_4P_3/graphite composite is clear.

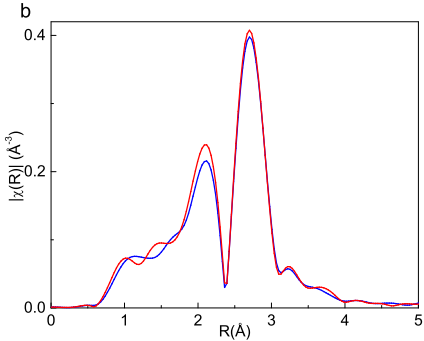

pure Sn_4P_3

Even at the 100^{th} delithiation, the Sn_4P_3/graphite composite measured *ex situ* is showing the same features as at the 3^{rd} cycle.

"In situ EXAFS-derived mechanism of highly reversible tin phosphide/graphite composite anode for Li-ion batteries," Y. Ding, Z. Li, E.V. Timofeeva, and C.U. Segre, *Adv. Energy Mater.* **8**, 1702134 (2018).

Sn_4P_3/graphite initial cycling

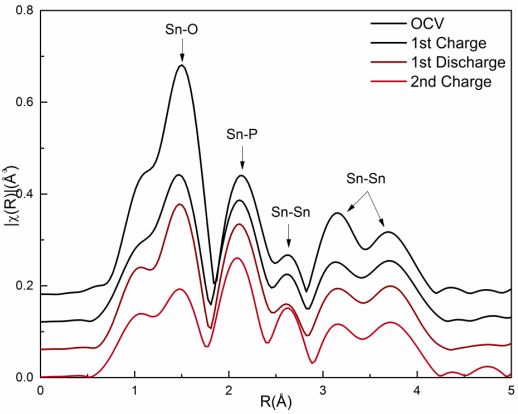

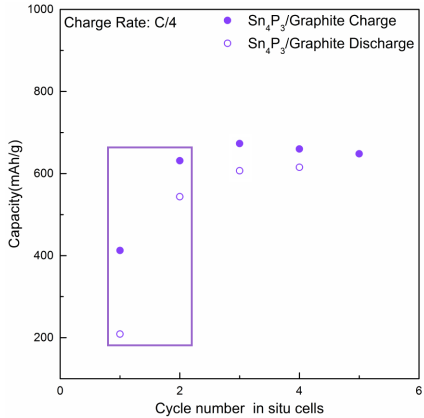

OCV spectrum fits well to Sn_4P_3 structure with an additional Sn-O path

Sn_4P_3 structure persists through first two cycles with possible enhancement of the Sn-Sn path at 2.6 Å

Sn_4P_3/graphite reversible cycling

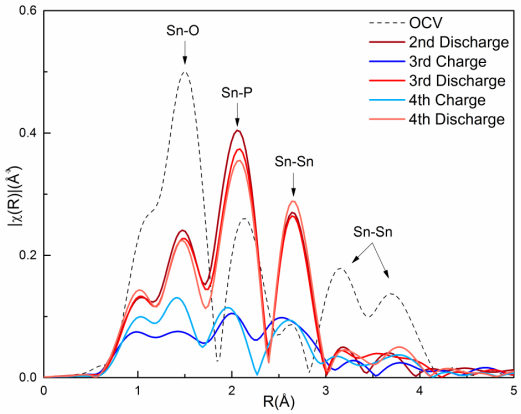

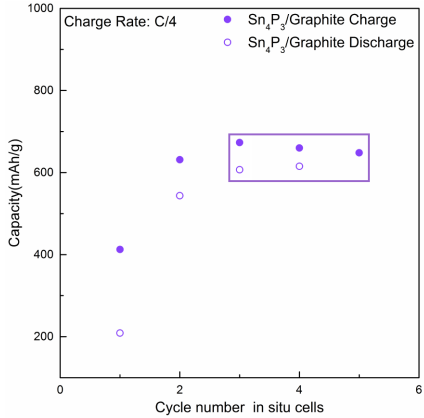

On third lithiation (charge) the Sn-P path is gone and only Sn-Li remains

Delithiation (discharge) produces Sn-P and Sn-Sn paths which are not those of Sn_4P_3 but are reversible

Example fits

Fit EXAFS for bond lengths and co-ordination numbers

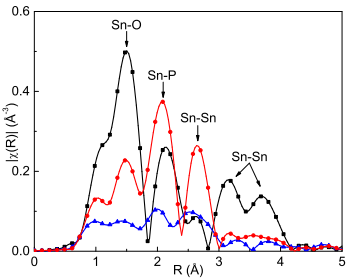

The Sn-O peak at OCV is due to ball milling, which introduces oxygen.

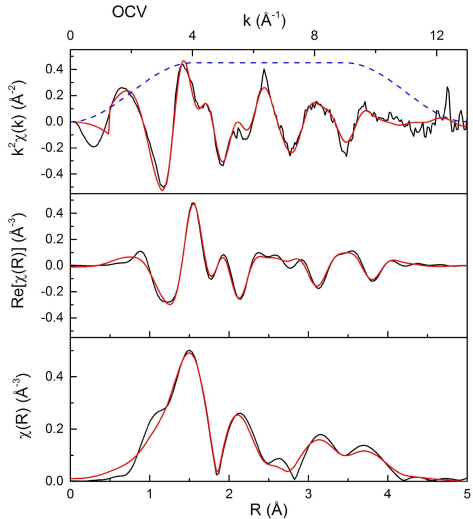

"In situ EXAFS-derived mechanism of highly reversible tin phosphide/graphite composite anode for Li-ion batteries," Y. Ding, Z. Li, E.V. Timofeeva, and C.U. Segre, *Adv. Energy Mater.* **8**, 1702134 (2018).

Example fits

Fit EXAFS for bond lengths and coordination numbers

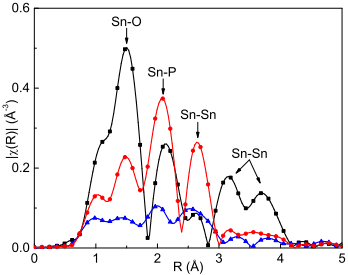

By the 3rd lithiated state, the EXAFS is dominated by Sn-Li paths at 2.7 Å and 3.0 Å.

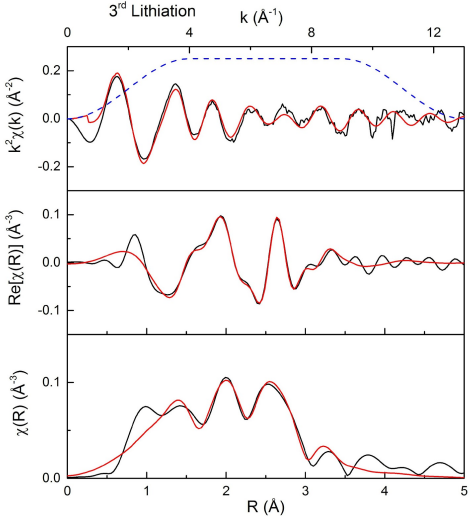

"In situ EXAFS-derived mechanism of highly reversible tin phosphide/graphite composite anode for Li-ion batteries," Y. Ding, Z. Li, E.V. Timofeeva, and C.U. Segre, *Adv. Energy Mater.* **8**, 1702134 (2018).

Example fits

Fit EXAFS for bond lengths and coordination numbers

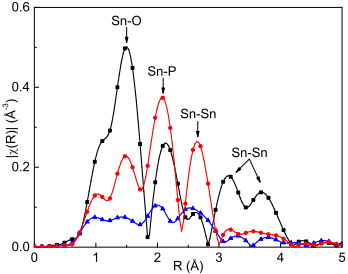

At the 3rd delithiation, the Sn-P path reappears but at a shorter distance, in an amorphous SnP_x phase.

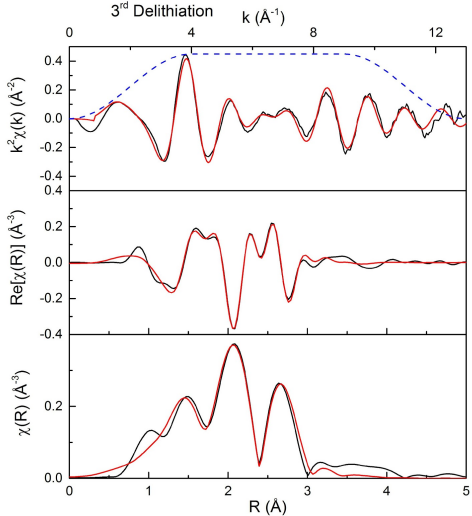

"In situ EXAFS-derived mechanism of highly reversible tin phosphide/graphite composite anode for Li-ion batteries," Y. Ding, Z. Li, E.V. Timofeeva, and C.U. Segre, *Adv. Energy Mater.* **8**, 1702134 (2018).

Sn_4P_3/graphite path lengths

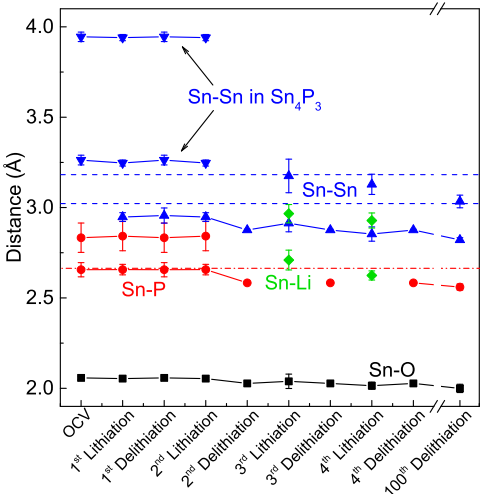

Y. Ding et al., "In situ EXAFS-derived mechanism of highly reversible tin phosphide/graphite composite anode for Li-ion batteries," Y. Ding, Z. Li, E.V. Timofeeva, and C.U. Segre, *Adv. Energy Mater.* **8**, 1702134 (2018).

Sn_4P_3/graphite path lengths

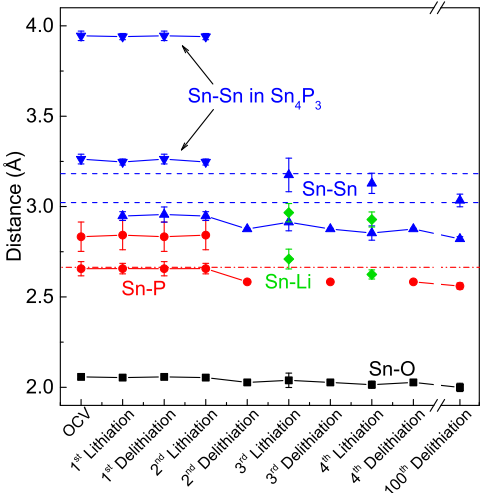

Sn-Sn distance close to those of metallic Sn indicate the presence of small Sn clusters which may never fully lithiate

Y. Ding et al., "In situ EXAFS-derived mechanism of highly reversible tin phosphide/graphite composite anode for Li-ion batteries," Y. Ding, Z. Li, E.V. Timofeeva, and C.U. Segre, *Adv. Energy Mater.* **8**, 1702134 (2018).

Sn_4P_3/graphite path lengths

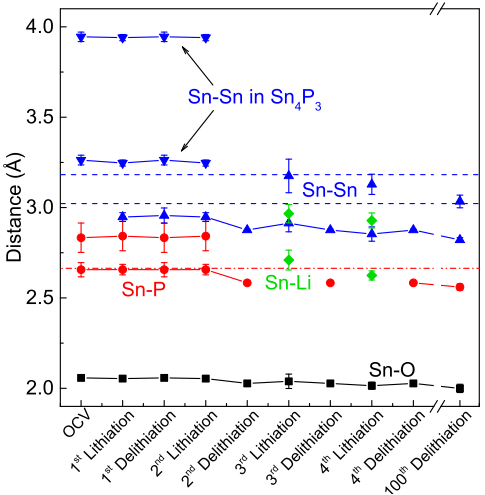

Sn-Sn distance close to those of metallic Sn indicate the presence of small Sn clusters which may never fully lithiate

Longer Sn-P distance characteristic of Sn_4P_3 is gone after initial conversion to the SnP_x amorphous phase is complete

Y. Ding et al., "In situ EXAFS-derived mechanism of highly reversible tin phosphide/graphite composite anode for Li-ion batteries," Y. Ding, Z. Li, E.V. Timofeeva, and C.U. Segre, *Adv. Energy Mater.* **8**, 1702134 (2018).

Sn_4P_3/graphite path lengths

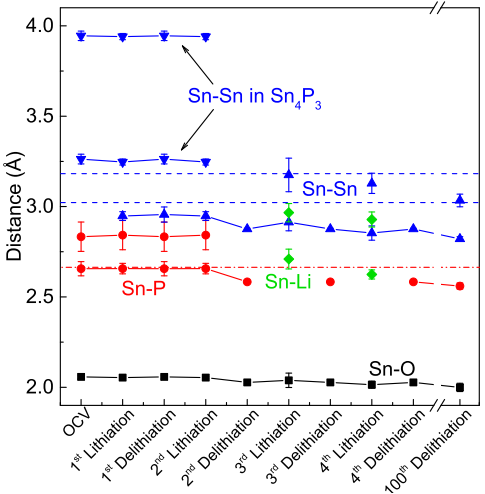

Sn-Sn distance close to those of metallic Sn indicate the presence of small Sn clusters which may never fully lithiate

Longer Sn-P distance characteristic of Sn_4P_3 is gone after initial conversion to the SnP_x amorphous phase is complete

Only 2 Sn-Li paths present in this material

Y. Ding et al., "In situ EXAFS-derived mechanism of highly reversible tin phosphide/graphite composite anode for Li-ion batteries," Y. Ding, Z. Li, E.V. Timofeeva, and C.U. Segre, *Adv. Energy Mater.* **8**, 1702134 (2018).

Sn_4P_3/graphite path lengths

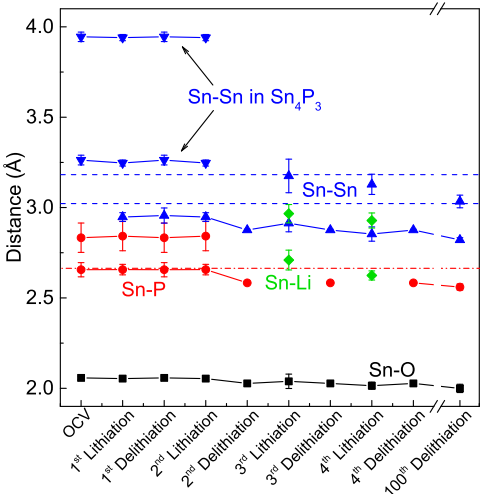

Sn-Sn distance close to those of metallic Sn indicate the presence of small Sn clusters which may never fully lithiate

Longer Sn-P distance characteristic of Sn_4P_3 is gone after initial conversion to the SnP_x amorphous phase is complete

Only 2 Sn-Li paths present in this material

Sn-O distances remain constant, likely indicative of surface contamination

Y. Ding et al., "In situ EXAFS-derived mechanism of highly reversible tin phosphide/graphite composite anode for Li-ion batteries," Y. Ding, Z. Li, E.V. Timofeeva, and C.U. Segre, *Adv. Energy Mater.* **8**, 1702134 (2018).

Sn_4P_3/graphite coordination numbers

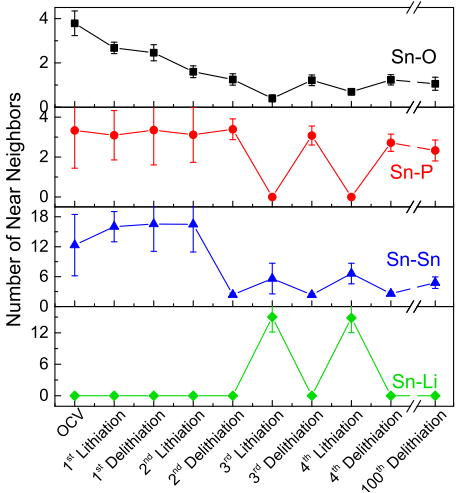

Sn-O neighbors decrease quickly, remaining small and partially reversible up to 100 cycles

Y. Ding et al., "In situ EXAFS-derived mechanism of highly reversible tin phosphide/graphite composite anode for Li-ion batteries," Y. Ding, Z. Li, E.V. Timofeeva, and C.U. Segre, *Adv. Energy Mater.* **8**, 1702134 (2018).

Sn_4P_3/graphite coordination numbers

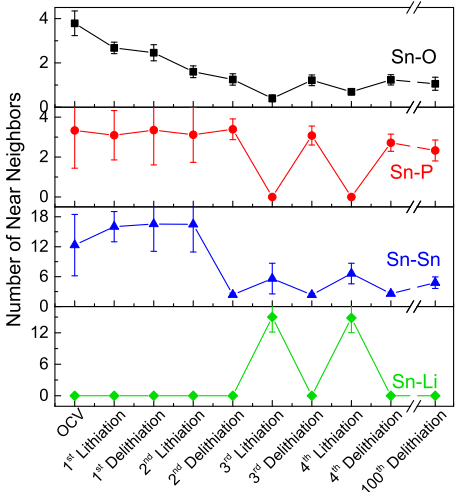

Sn-O neighbors decrease quickly, remaining small and partially reversible up to 100 cycles

Sn-P reversible after initial conversion with a slow decrease which correlates to capacity loss

Y. Ding et al., "In situ EXAFS-derived mechanism of highly reversible tin phosphide/graphite composite anode for Li-ion batteries," Y. Ding, Z. Li, E.V. Timofeeva, and C.U. Segre, *Adv. Energy Mater.* **8**, 1702134 (2018).

Sn_4P_3/graphite coordination numbers

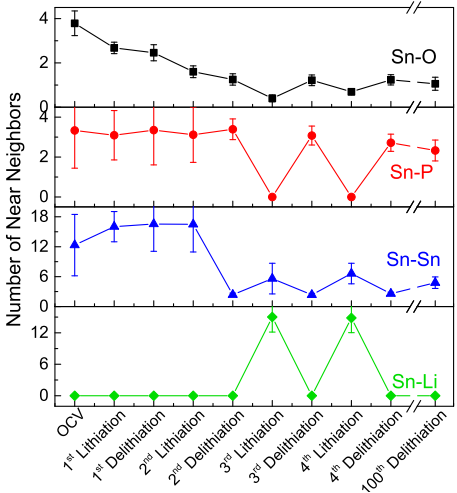

Sn-O neighbors decrease quickly, remaining small and partially reversible up to 100 cycles

Sn-P reversible after initial conversion with a slow decrease which correlates to capacity loss

Very small Sn-Sn metallic clusters present throughout

Y. Ding et al., "In situ EXAFS-derived mechanism of highly reversible tin phosphide/graphite composite anode for Li-ion batteries," Y. Ding, Z. Li, E.V. Timofeeva, and C.U. Segre, *Adv. Energy Mater.* **8**, 1702134 (2018).

Sn_4P_3/graphite coordination numbers

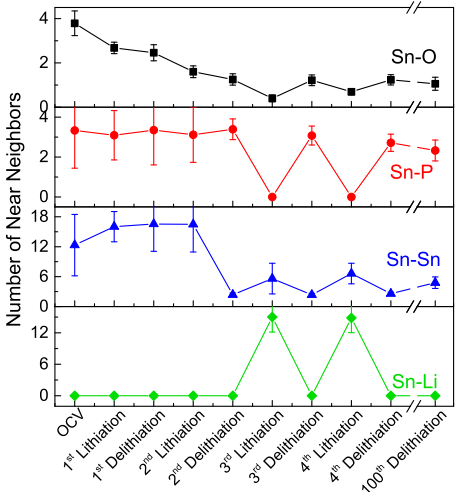

Sn-O neighbors decrease quickly, remaining small and partially reversible up to 100 cycles

Sn-P reversible after initial conversion with a slow decrease which correlates to capacity loss

Very small Sn-Sn metallic clusters present throughout

The $\sim$3.3 Sn-P neighbors in the delithiated state indicate a possibly tetrahedral Sn coordination in SnP_x

Y. Ding et al., "In situ EXAFS-derived mechanism of highly reversible tin phosphide/graphite composite anode for Li-ion batteries," Y. Ding, Z. Li, E.V. Timofeeva, and C.U. Segre, *Adv. Energy Mater.* **8**, 1702134 (2018).

Third cycle dynamic snapshot

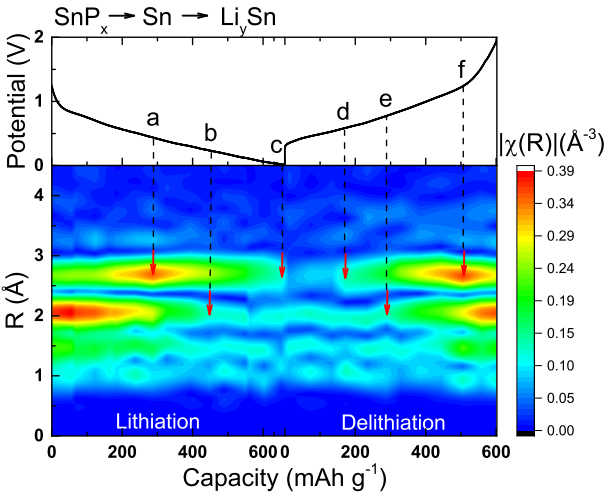

"In situ EXAFS-derived mechanism of highly reversible tin phosphide/graphite composite anode for Li-ion batteries," Y. Ding, Z. Li, E.V. Timofeeva, and C.U. Segre, *Adv. Energy Mater.* **8**, 1702134 (2018).

Third cycle dynamic snapshot

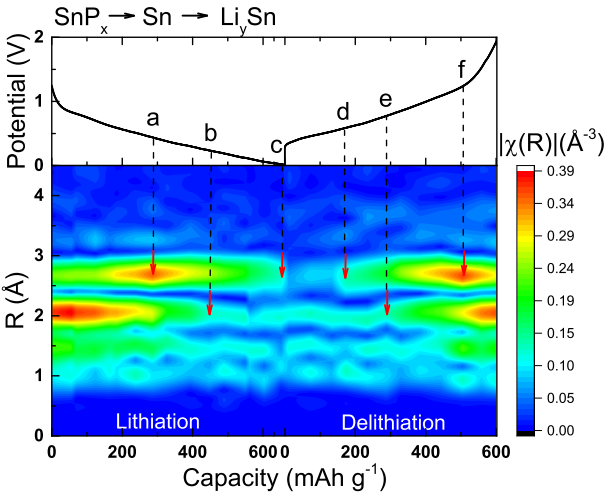

Amorphous SnP_x fully formed at start of 3^{rd} cycle

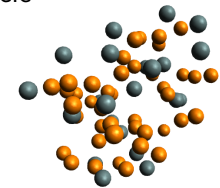

"In situ EXAFS-derived mechanism of highly reversible tin phosphide/graphite composite anode for Li-ion batteries," Y. Ding, Z. Li, E.V. Timofeeva, and C.U. Segre, *Adv. Energy Mater.* **8**, 1702134 (2018).

Third cycle dynamic snapshot

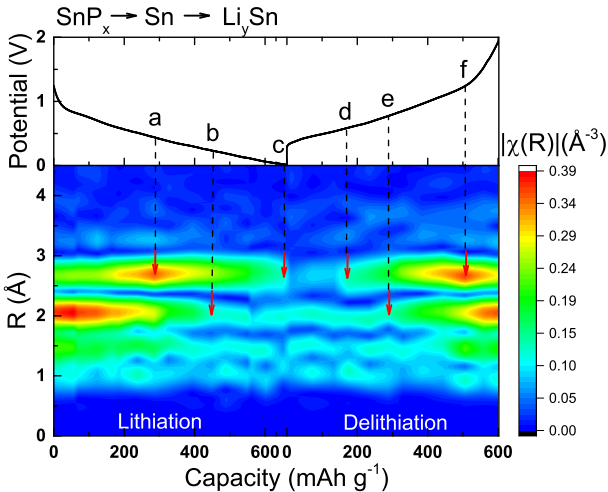

Amorphous SnP_x fully formed at start of 3^{rd} cycle

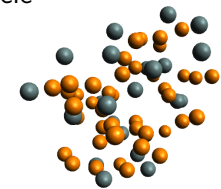

a. Sn lithiating

"In situ EXAFS-derived mechanism of highly reversible tin phosphide/graphite composite anode for Li-ion batteries," Y. Ding, Z. Li, E.V. Timofeeva, and C.U. Segre, *Adv. Energy Mater.* **8**, 1702134 (2018).

Third cycle dynamic snapshot

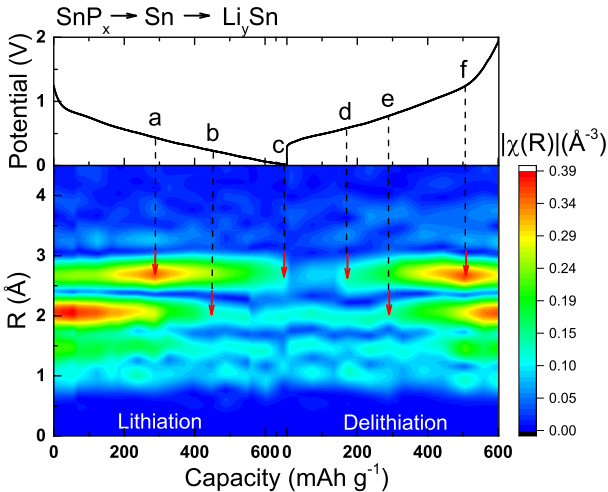

Amorphous SnP_x fully formed at start of 3^{rd} cycle

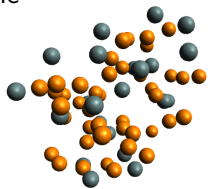

a. Sn lithiating
b. SnP_x all gone

"In situ EXAFS-derived mechanism of highly reversible tin phosphide/graphite composite anode for Li-ion batteries," Y. Ding, Z. Li, E.V. Timofeeva, and C.U. Segre, *Adv. Energy Mater.* **8**, 1702134 (2018).

Third cycle dynamic snapshot

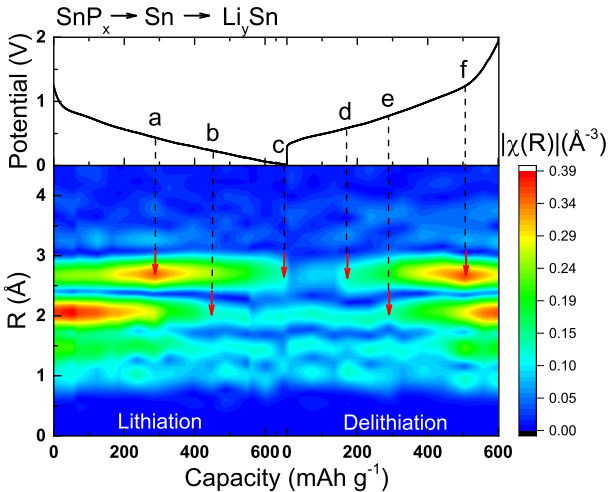

Amorphous SnP_x fully formed at start of 3^{rd} cycle

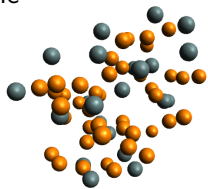

a. Sn lithiating
b. SnP_x all gone
c. full lithiation

"In situ EXAFS-derived mechanism of highly reversible tin phosphide/graphite composite anode for Li-ion batteries," Y. Ding, Z. Li, E.V. Timofeeva, and C.U. Segre, *Adv. Energy Mater.* **8**, 1702134 (2018).

Third cycle dynamic snapshot

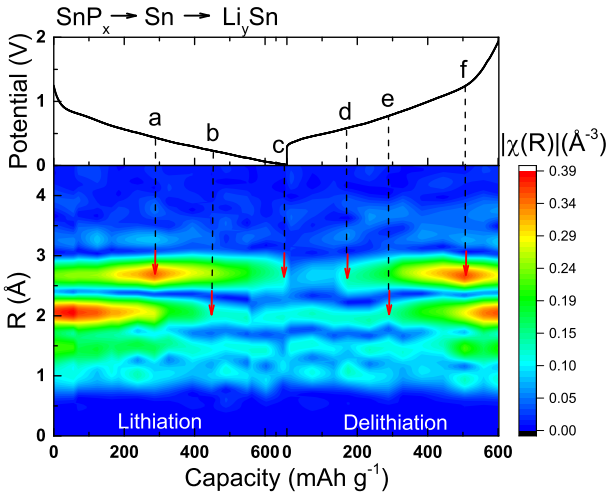

Amorphous SnP_x fully formed at start of 3^{rd} cycle

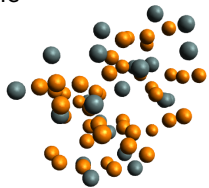

a. Sn lithiating
b. SnP_x all gone
c. full lithiation
d. Sn appears

"In situ EXAFS-derived mechanism of highly reversible tin phosphide/graphite composite anode for Li-ion batteries," Y. Ding, Z. Li, E.V. Timofeeva, and C.U. Segre, *Adv. Energy Mater.* **8**, 1702134 (2018).

Third cycle dynamic snapshot

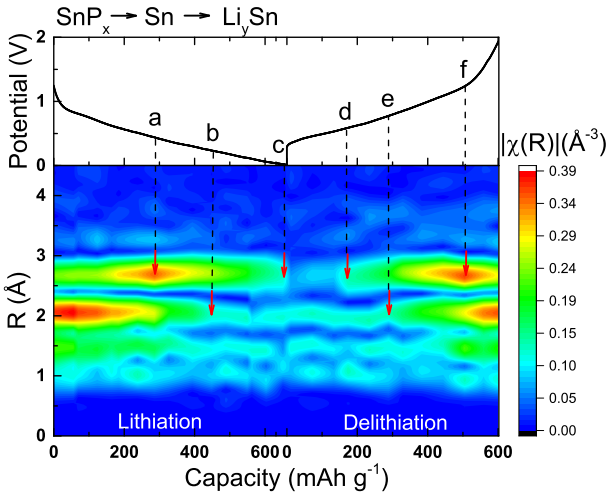

Amorphous SnP_x fully formed at start of 3^{rd} cycle

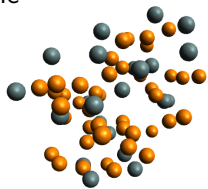

a. Sn lithiating
b. SnP_x all gone
c. full lithiation
d. Sn appears
e. SnP_x appears

"In situ EXAFS-derived mechanism of highly reversible tin phosphide/graphite composite anode for Li-ion batteries," Y. Ding, Z. Li, E.V. Timofeeva, and C.U. Segre, *Adv. Energy Mater.* **8**, 1702134 (2018).

Third cycle dynamic snapshot

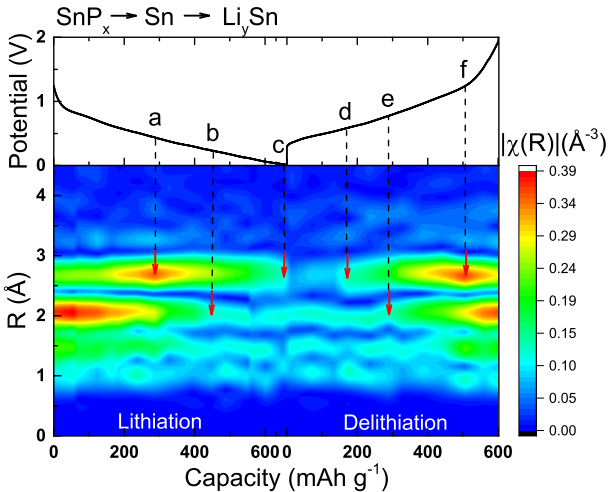

Amorphous SnP_x fully formed at start of 3^{rd} cycle

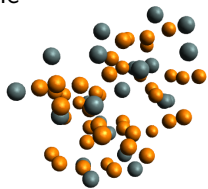

a. Sn lithiating
b. SnP_x all gone
c. full lithiation
d. Sn appears
e. SnP_x appears
f. Sn delithiated

"In situ EXAFS-derived mechanism of highly reversible tin phosphide/graphite composite anode for Li-ion batteries," Y. Ding, Z. Li, E.V. Timofeeva, and C.U. Segre, *Adv. Energy Mater.* **8**, 1702134 (2018).

The photoemission process

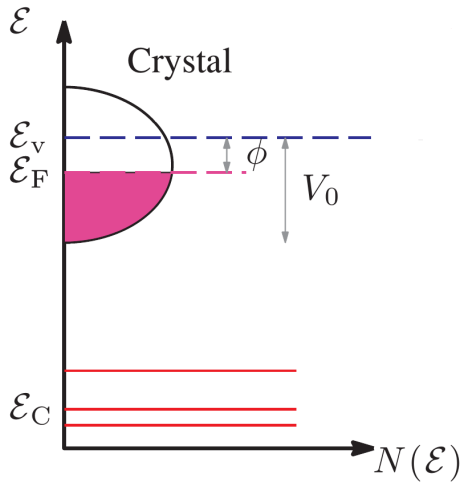

Photoemission is the complement to XAFS. It probes the filled states below the Fermi level

The photoemission process

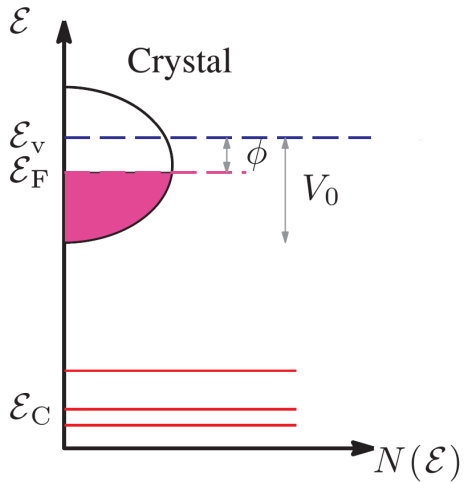

Photoemission is the complement to XAFS. It probes the filled states below the Fermi level

The dispersion relation of electrons in a solid, $\mathcal{E}(\vec{q})$ can be probed by angle resolved photoemission since both the kinetic energy, $\mathcal{E}_{kin}$, and the angle, θ are measured

The photoemission process

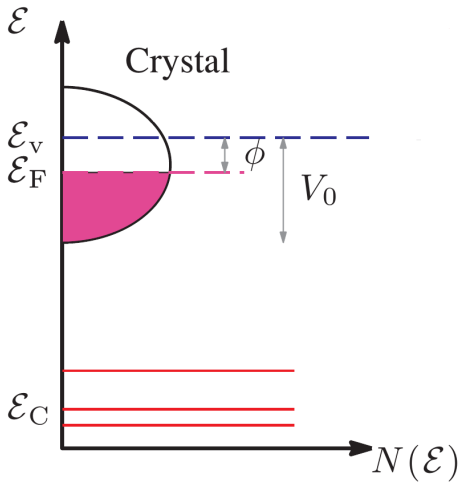

Photoemission is the complement to XAFS. It probes the filled states below the Fermi level

The dispersion relation of electrons in a solid, $\mathcal{E}(\vec{q})$ can be probed by angle resolved photoemission since both the kinetic energy, $\mathcal{E}_{kin}$, and the angle, θ are measured

$$\mathcal{E}_{kin},\ \theta \longrightarrow \mathcal{E}(\vec{q})$$

The photoemission process

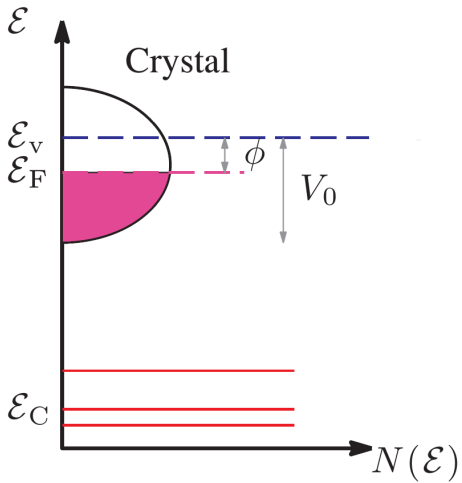

Photoemission is the complement to XAFS. It probes the filled states below the Fermi level

The dispersion relation of electrons in a solid, $\mathcal{E}(\vec{q})$ can be probed by angle resolved photoemission since both the kinetic energy, $\mathcal{E}_{kin}$, and the angle, θ are measured

$$\mathcal{E}_{kin},\ \theta \longrightarrow \mathcal{E}(\vec{q})$$

The core levels are tightly bound at an energy $\mathcal{E}_C$ below the Fermi level

The photoemission process

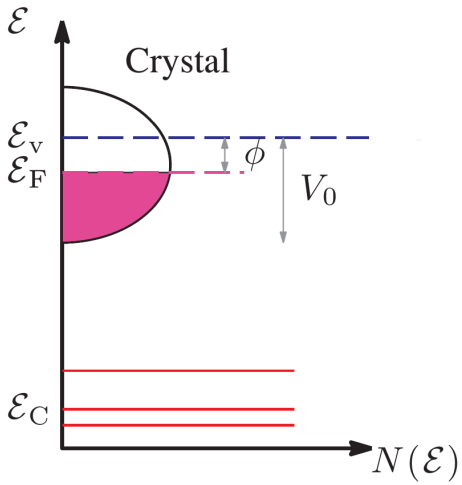

$$\phi = \mathcal{E}_v - \mathcal{E}_F$$

Photoemission is the complement to XAFS. It probes the filled states below the Fermi level

The dispersion relation of electrons in a solid, $\mathcal{E}(\vec{q})$ can be probed by angle resolved photoemission since both the kinetic energy, $\mathcal{E}_{kin}$, and the angle, θ are measured

$$\mathcal{E}_{kin},\ \theta \longrightarrow \mathcal{E}(\vec{q})$$

The core levels are tightly bound at an energy $\mathcal{E}_C$ below the Fermi level

The work function, ϕ, is the minimum energy required to promote an electron from the top of the valence band at the Fermi energy, $\mathcal{E}_F$, to the vacuum energy, $\mathcal{E}_v$

The photoemission process

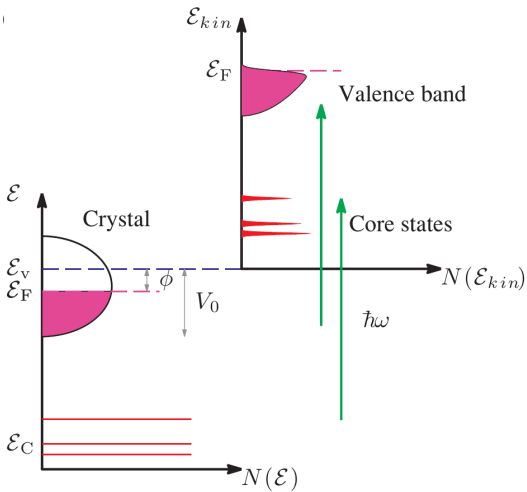

With the incident photon energy, $\hbar\omega$, held constant, an analyzer is used to measure the kinetic energy, $\mathcal{E}_{kin}$, of the photoelectrons emitted from the surface of the sample

The photoemission process

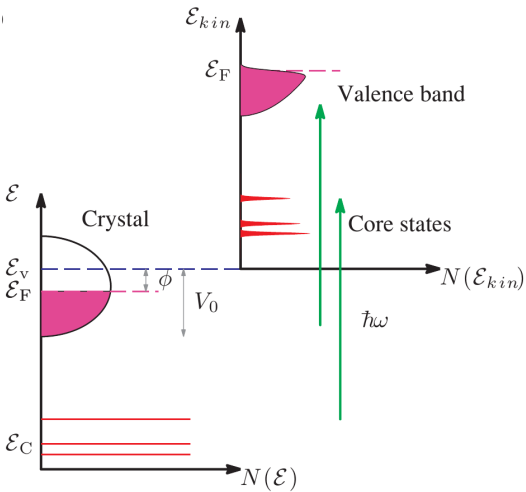

With the incident photon energy, $\hbar\omega$, held constant, an analyzer is used to measure the kinetic energy, $\mathcal{E}_{kin}$, of the photoelectrons emitted from the surface of the sample

if $\mathcal{E}_i$ is the initial energy of the electron, the binding energy, $\mathcal{E}_B$ is

The photoemission process

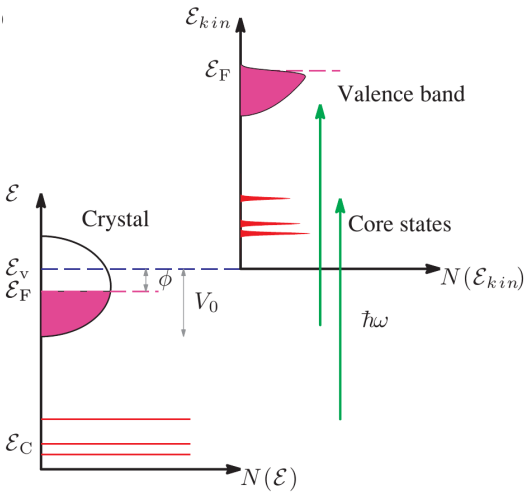

With the incident photon energy, $\hbar\omega$, held constant, an analyzer is used to measure the kinetic energy, $\mathcal{E}_{kin}$, of the photoelectrons emitted from the surface of the sample

if $\mathcal{E}_i$ is the initial energy of the electron, the binding energy, $\mathcal{E}_B$ is

$$\mathcal{E}_B = \mathcal{E}_F - \mathcal{E}_i$$

The photoemission process

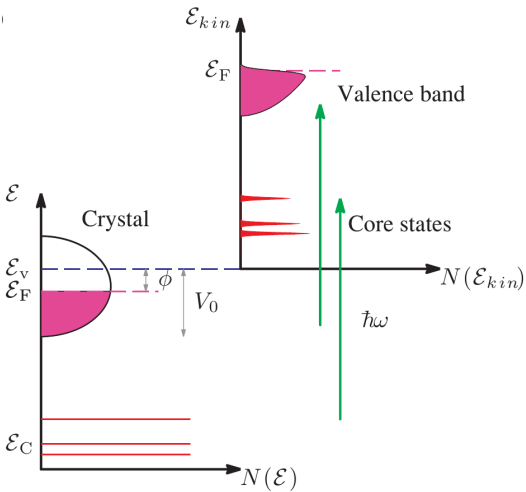

With the incident photon energy, $\hbar\omega$, held constant, an analyzer is used to measure the kinetic energy, $\mathcal{E}_{kin}$, of the photoelectrons emitted from the surface of the sample

if $\mathcal{E}_i$ is the initial energy of the electron, the binding energy, $\mathcal{E}_B$ is

$$\mathcal{E}_B = \mathcal{E}_F - \mathcal{E}_i$$

and the measured kinetic energy gives the binding energy

The photoemission process

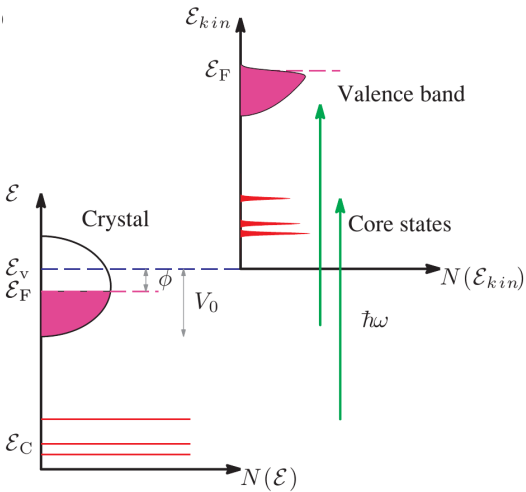

With the incident photon energy, $\hbar\omega$, held constant, an analyzer is used to measure the kinetic energy, $\mathcal{E}_{kin}$, of the photoelectrons emitted from the surface of the sample

if $\mathcal{E}_i$ is the initial energy of the electron, the binding energy, $\mathcal{E}_B$ is

$$\mathcal{E}_B = \mathcal{E}_F - \mathcal{E}_i$$

and the measured kinetic energy gives the binding energy

$$\mathcal{E}_{kin} = \frac{\hbar^2 q_v^2}{2m}$$

The photoemission process

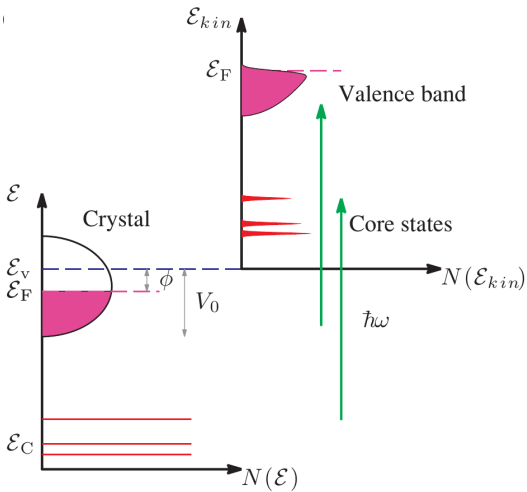

With the incident photon energy, $\hbar\omega$, held constant, an analyzer is used to measure the kinetic energy, $\mathcal{E}_{kin}$, of the photoelectrons emitted from the surface of the sample

if $\mathcal{E}_i$ is the initial energy of the electron, the binding energy, $\mathcal{E}_B$ is

$$\mathcal{E}_B = \mathcal{E}_F - \mathcal{E}_i$$

and the measured kinetic energy gives the binding energy

$$\mathcal{E}_{kin} = \frac{\hbar^2 q_v^2}{2m} = \hbar\omega - \phi - \mathcal{E}_B$$

The photoemission process

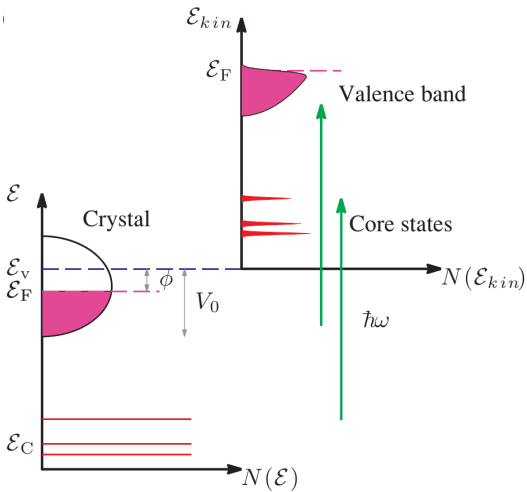

With the incident photon energy, $\hbar\omega$, held constant, an analyzer is used to measure the kinetic energy, $\mathcal{E}_{kin}$, of the photoelectrons emitted from the surface of the sample

if $\mathcal{E}_i$ is the initial energy of the electron, the binding energy, $\mathcal{E}_B$ is

$$\mathcal{E}_B = \mathcal{E}_F - \mathcal{E}_i$$

and the measured kinetic energy gives the binding energy

$$\mathcal{E}_{kin} = \frac{\hbar^2 q_v^2}{2m} = \hbar\omega - \phi - \mathcal{E}_B$$

the maximum kinetic energy measured is thus related to the Fermi energy

The photoemission process

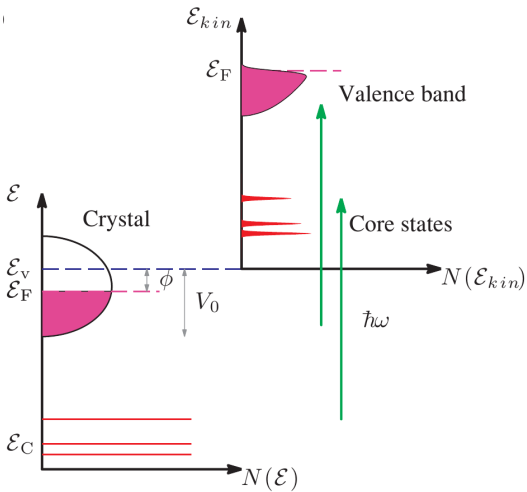

With the incident photon energy, $\hbar\omega$, held constant, an analyzer is used to measure the kinetic energy, $\mathcal{E}_{kin}$, of the photoelectrons emitted from the surface of the sample

if $\mathcal{E}_i$ is the initial energy of the electron, the binding energy, $\mathcal{E}_B$ is

$$\mathcal{E}_B = \mathcal{E}_F - \mathcal{E}_i$$

and the measured kinetic energy gives the binding energy

$$\mathcal{E}_{kin} = \frac{\hbar^2 q_v^2}{2m} = \hbar\omega - \phi - \mathcal{E}_B$$

the maximum kinetic energy measured is thus related to the Fermi energy

the core states are used to fingerprint the chemical composition of the sample

Hemispherical mirror analyzer

The electric field between the two hemispheres of radius R_1 and R_2 has a R^2 dependence from the center of the hemispheres

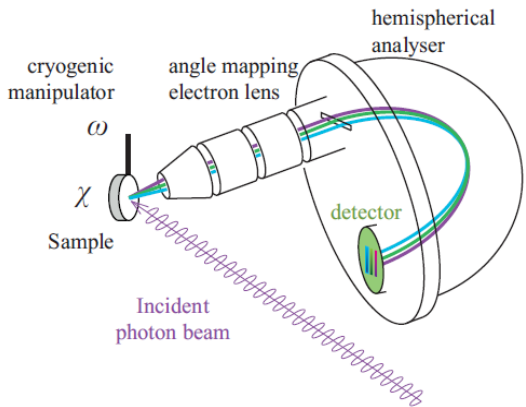

Hemispherical mirror analyzer

The electric field between the two hemispheres of radius R_1 and R_2 has a R^2 dependence from the center of the hemispheres

Electrons with $\mathcal{E}_0$, called the "pass energy", will follow a circular path of radius

$$R_0 = (R_1 + R_2)/2$$

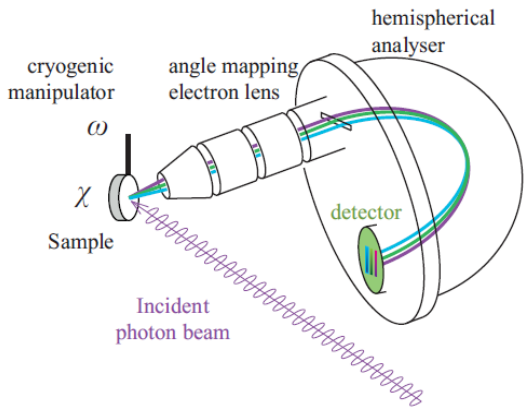

Hemispherical mirror analyzer

The electric field between the two hemispheres of radius R_1 and R_2 has a R^2 dependence from the center of the hemispheres

Electrons with $\mathcal{E}_0$, called the "pass energy", will follow a circular path of radius

$$R_0 = (R_1 + R_2)/2$$

Electrons with lower energy will fall inside this circular path while those with higher energy will fall outside

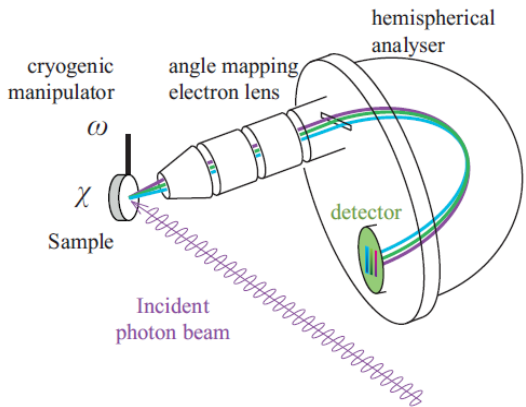

Hemispherical mirror analyzer

The electric field between the two hemispheres of radius R_1 and R_2 has a R^2 dependence from the center of the hemispheres

Electrons with $\mathcal{E}_0$, called the "pass energy", will follow a circular path of radius

$$R_0 = (R_1 + R_2)/2$$

Electrons with lower energy will fall inside this circular path while those with higher energy will fall outside

Electrons with different azimuthal exit angles ω will map to different positions on the 2D detector